Conflicting evidence for HIV enrichment in CD32$^+$ CD4 T cells

ARISING FROM B. Descours et al. *Nature* **543**, 564–567 (2017); https://doi.org/10.1038/nature21710

Descours and colleagues[1] reported a marked enrichment for HIV among CD32a$^+$ CD4 T cells in people receiving anti-retroviral therapy (ART). This tiny CD32a$^+$ population (0.012% of all blood CD4 T cells) contained a median of 0.56 HIV DNA genomes per cell, and accounted for 26.8–86.3% of HIV DNA in CD4 T cells, thus suggesting that targeting CD32a$^+$ CD4 T cells might help to clear HIV reservoirs in vivo. Here, we report our unsuccessful attempts to confirm these findings. There is a Reply to this Comment by Descours, B. et al. *Nature* **561**, https://doi.org/10.1038/s41586-018-0496-1 (2018).

We first used fluorescence-activated cell sorting (FACS) to sort CD4 T cells with high, intermediate and low levels of CD32 staining (CD32^{hi}, CD32^{int} and CD32^{lo}, respectively) from 10 individuals with chronic HIV infection who were receiving ART (mean duration, 8.8 years; range, 2.7–15). We used cell-staining reagents and gating techniques that matched those used by Descours et al.[1] (see Supplementary Methods and Extended Data Fig. 1). As shown in Fig. 1a, we detected no enrichment for HIV DNA in the CD32^{hi} or CD32^{int} CD4 T cells. Moreover, the CD32^{hi} and CD32^{int} subsets combined accounted for no more than 3% of all HIV DNA copies within circulating CD4 T cells in any of the 10 study participants (Fig. 1b). Post-sort flow cytometry of CD32^{hi} and CD32^{int} populations showed heterogeneous patterns that suggested the formation of T cell–B cell or T cell–monocyte conjugates as the origin of most CD32^{hi} or CD32^{int} CD4 T cells, with separation of these conjugates during sorting (Extended Data Fig. 2).

To rule out the possibility that we had inadvertently obtained false negative results either by excluding HIV-infected, CD32$^+$ CD4 T cells using tight light scatter gates or by failing to exclude non-T-cell contaminants, we performed parallel sorts on the same 10 samples using an alternative gating scheme. We used a more inclusive light scatter gate as well as markers for B cells, monocytes, dendritic cells and natural killer cells (Extended Data Fig. 3). Events that were CD3$^+$ were separated into fractions that were positive for B cell markers (T–B), positive for one or more other non-CD4-T-cell markers (T–other), or negative for all of these, positive for CD4, and CD32^{hi}, CD32^{int} or CD32^{lo}. Neither CD32^{hi} nor CD32^{int} CD4 T cells were enriched for HIV DNA (Fig. 2a). Similarly, we detected no enrichment for HIV DNA in the T–B and T–other populations (Fig. 2a). In each of the 10 participants, at least 96% of all HIV DNA copies occurred in conventional CD32^{lo} cells (Fig. 2b). Post-sort flow cytometry suggested that most events bearing both T-cell and non-CD4-T-cell markers again represented cell–cell conjugates, and also showed that most remaining CD32^{hi} CD4 T cells did not reproducibly show a high CD32 signal after sorting (Extended Data Fig. 4). This was in contrast to conventional CD32^{lo} cells, which were uniformly pure in post-sort analyses across participants. In a second group of four individuals whose peripheral blood mononuclear cells (PBMCs) were sorted without previous cryopreservation (Extended Data Fig. 5a), we again found no enrichment for HIV DNA based on CD32 expression (Extended Data Fig. 5b), and also observed that HIV DNA sequences in CD32$^+$ CD4 T cells were genetically intermingled with HIV DNA sequences in other CD4 T cells (Extended Data Fig. 5c).

Overall, our studies showed no enrichment for HIV DNA in CD32$^+$ CD4 T cells, and also raised questions about the source of the CD32 labelling on these cells. We propose that the CD32 expression associated previously with CD4 T cells could have arisen from adherent non-T-cells or cellular material bearing this marker, and that conjugates containing HIV-infected CD4 T cells could be differentially produced and/or recovered in different laboratories with different sample processing and FACS practices. It is important to acknowledge that these considerations do not explain the discrepancy between the Descours et al. study[1] and ours in the quantities of HIV DNA detected within CD3$^+$CD4$^+$CD32$^+$ sorted material. Nevertheless, we wish to emphasize that our findings do not support targeting CD32 molecules on CD4 T cells in emerging HIV cure strategies.

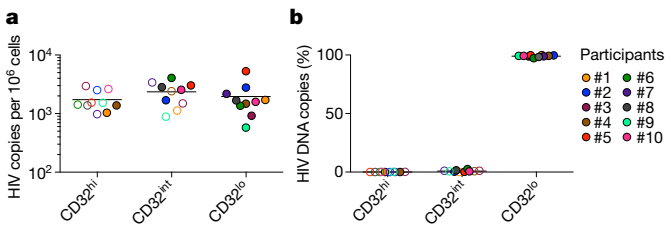

Fig. 1 | Levels of HIV DNA in CD32^{hi}, CD32^{int} and CD32^{lo} CD4 T cells, sorted from PBMCs of 10 ART-treated participants, as in Descours et al.[1]. **a**, Copies of HIV DNA per million sorted cells. **b**, Percentages of all HIV DNA copies detected in blood CD4 T cells that were detected within each subset, calculated by adjusting values in **a** for the relative proportions of these subsets in FACS data. In all figures, horizontal bars denote median values, and open symbols indicate detection limits for measurements in which HIV DNA was not detected.

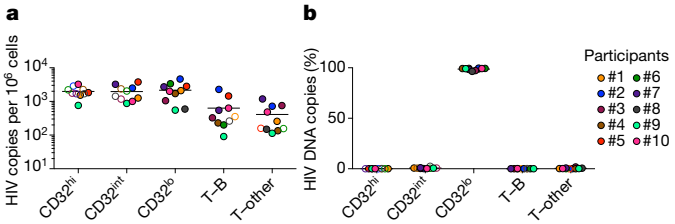

Fig. 2 | Levels of HIV DNA in CD32^{hi}, CD32^{int} and CD32^{lo} CD4 T cells, sorted using alternative gating. The samples from Fig. 1 were sorted using alternative gating in which T cells bearing markers of B cells (T–B) or other non-CD4-T-cell lineages (T–other) were first collected in separate tubes. **a**, Copies of HIV DNA per million sorted cells. **b**, Percentages of all HIV DNA copies detected in blood cells that were detected within each subset, calculated by adjusting values in **a** for the relative proportions of these subsets in FACS data.

Methods

Participant recruitment and informed consent were performed under Institutional Review Board (IRB)-approved protocols at the US National Institutes of Health (NIH). For FACS, whole PBMCs were stained with monoclonal antibodies matching those used by Descours et al.[1] (see Supplementary Methods) and sorted on a BD FACSAria. To evaluate purity, a portion of each population was re-analysed on the flow cytometer after sorting. Virus DNA copies in sorted cells were enumerated by fluorescence-assisted clonal amplification[2]. DNA recovery was quantified by albumin (*ALB*) quantitative PCR. Because the FUN-2 monoclonal antibody used

by Descours et al.[1] and in our study may recognize both CD32a and CD32b, we refer to cells staining with this monoclonal antibody as $CD32^{+}$.

Data availability. All DNA sequences in this manuscript (analysed in Extended Data Fig. 5) have been deposited in GenBank under accession numbers MH080310–MH080572.

Liliana Pérez[1], Jodi Anderson[2], Jeffrey Chipman[3], Ann Thorkelson[2], Tae-Wook Chun[4], Susan Moir[4], Ashley T. Haase[5], Daniel C. Douek[6], Timothy W. Schacker[2,7] & Eli A. Boritz[1,7]*

[1]Virus Persistence and Dynamics Section, Vaccine Research Center, National Institute of Allergy and Infectious Diseases, National Institutes of Health, Bethesda, MD, USA. [2]Division of Infectious Diseases, University of Minnesota, Minneapolis, MN, USA. [3]Department of Surgery, University of Minnesota, Minneapolis, MN, USA. [4]Laboratory of Immunoregulation, National Institute of Allergy and Infectious Disease, National Institutes of Health, Bethesda, MD, USA. [5]Department of Microbiology and Immunology, University of Minnesota, Minneapolis, MN, USA. [6]Human Immunology Section, Vaccine Research Center, National Institute of Allergy and Infectious Diseases, National Institutes of Health, Bethesda, MD, USA. [7]These authors jointly supervised this work: Timothy W. Schacker, Eli A. Boritz. *e-mail: boritze@mail.nih.gov

Received: 11 October 2017; Accepted: 20 March 2018;
Published online 19 September 2018.

1. Descours, B. et al. CD32a is a marker of a CD4 T-cell HIV reservoir harbouring replication-competent proviruses. *Nature* **543**, 564–567 (2017).
2. Boritz, E. A. et al. Multiple origins of virus persistence during natural control of HIV infection. *Cell* **166**, 1004–1015 (2016).

Author contributions Data generation and analysis: L.P., J.A., T.W.S. and E.A.B. Study design and oversight: L.P., A.T.H., D.C.D., T.W.S. and E.A.B. Participant cohort and sample management: J.A., J.C., A.T., T.W.C., S.M. and T.W.S. Manuscript preparation: L.P., A.T.H., D.C.D., T.W.S. and E.A.B.

Competing interests Declared none.

Additional information
Extended data accompanies this Comment.
Supplementary information accompanies this Comment.
Reprints and permissions information is available at http://www.nature.com/reprints.
Correspondence and requests for materials should be addressed to E.A.B.

https://doi.org/10.1038/s41586-018-0493-4

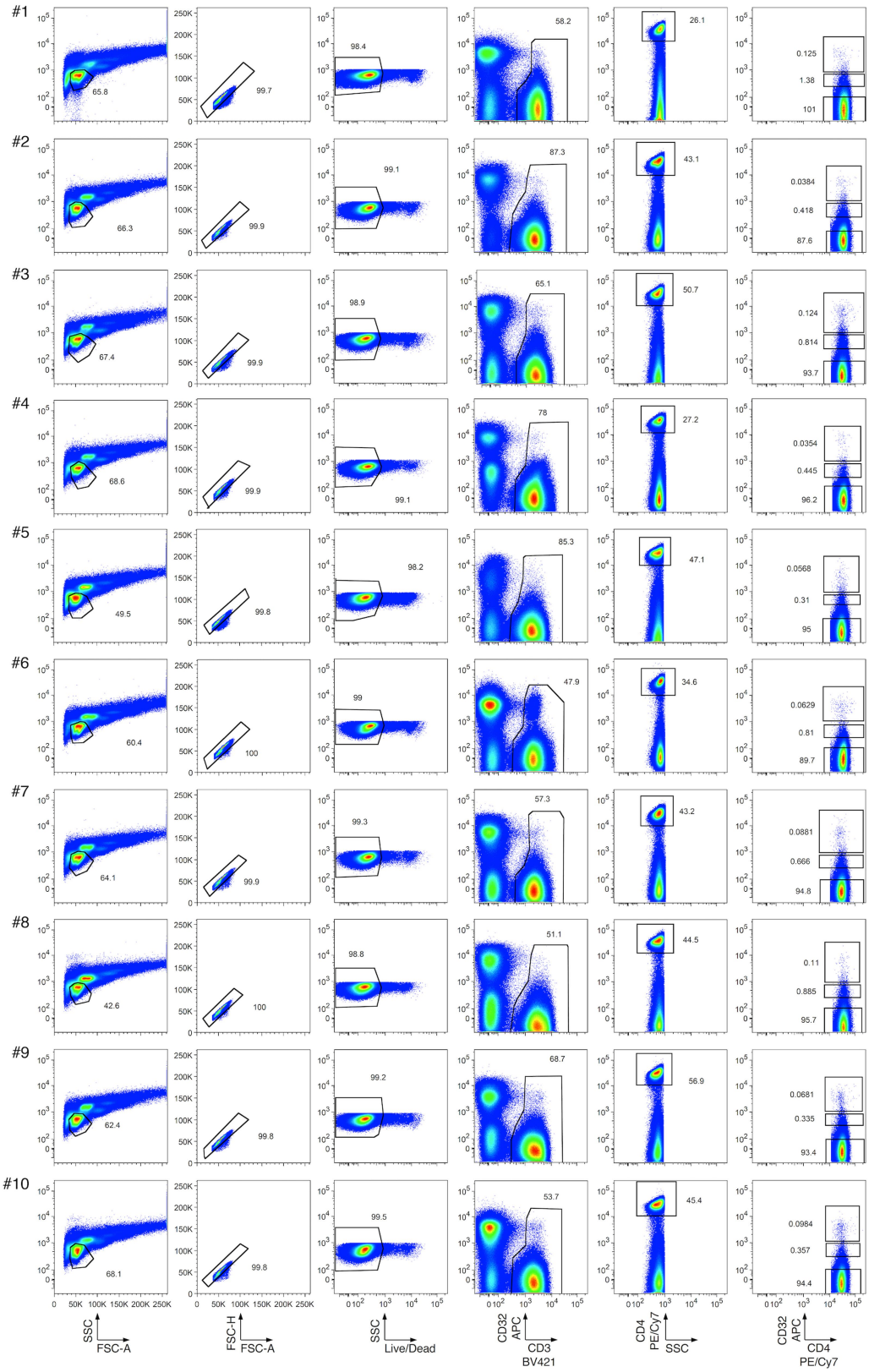

Extended Data Fig. 1 | Flow cytometry of CD32^{hi}, CD32^{int} and CD32^{lo} CD4 T cell populations from PBMCs. Single lymphocytes (first two columns) that were viable (third column), CD3^{+} (fourth column), CD4^{+} (fifth column), and CD32^{hi}, CD32^{int} or CD32^{lo} (sixth column) were sorted as described in Descours et al.[1].

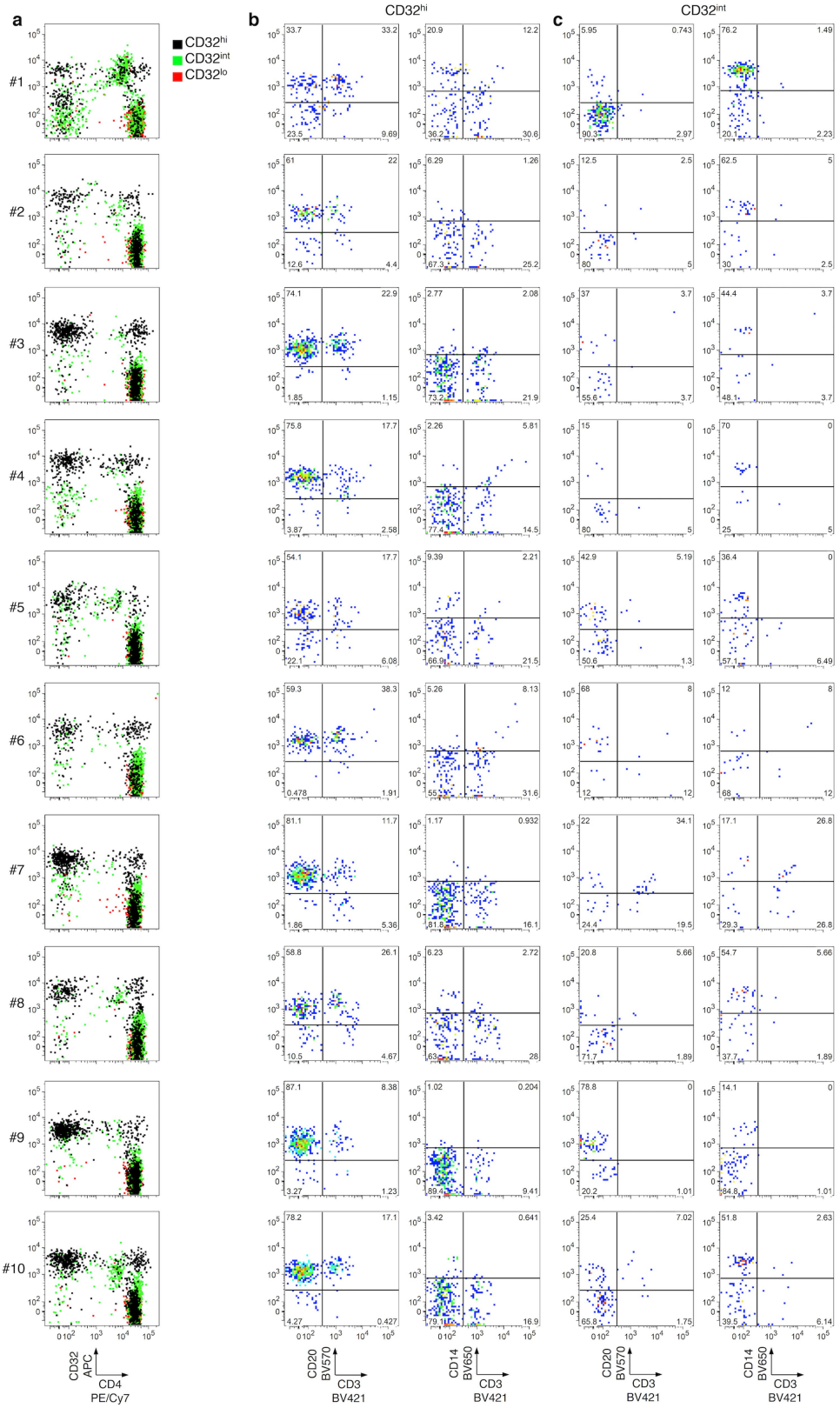

Extended Data Fig. 2 | Post-sort flow cytometry of CD3$^+$CD4$^+$ subsets that were CD32^{hi}, CD32^{int} or CD32^{lo}. Cells were sorted as in Extended Data Fig. 1. **a**, Overlay plots of CD32 and CD4 expression by cells in CD32^{hi}, CD32^{int} and CD32^{lo} sorted populations. Note the heterogeneous pattern of cells from the CD32^{hi} and CD32^{int} populations. **b**, **c**, CD20, CD14 and CD3 staining in the CD32$^+$ cells from the CD32^{hi} (**b**) and the CD32^{int} (**c**) subsets. Note the large proportions of all CD32$^+$ cells bearing surface markers consistent with B cells (CD20$^+$CD3$^-$) or monocytes (CD14$^+$CD3$^-$) after sorting.

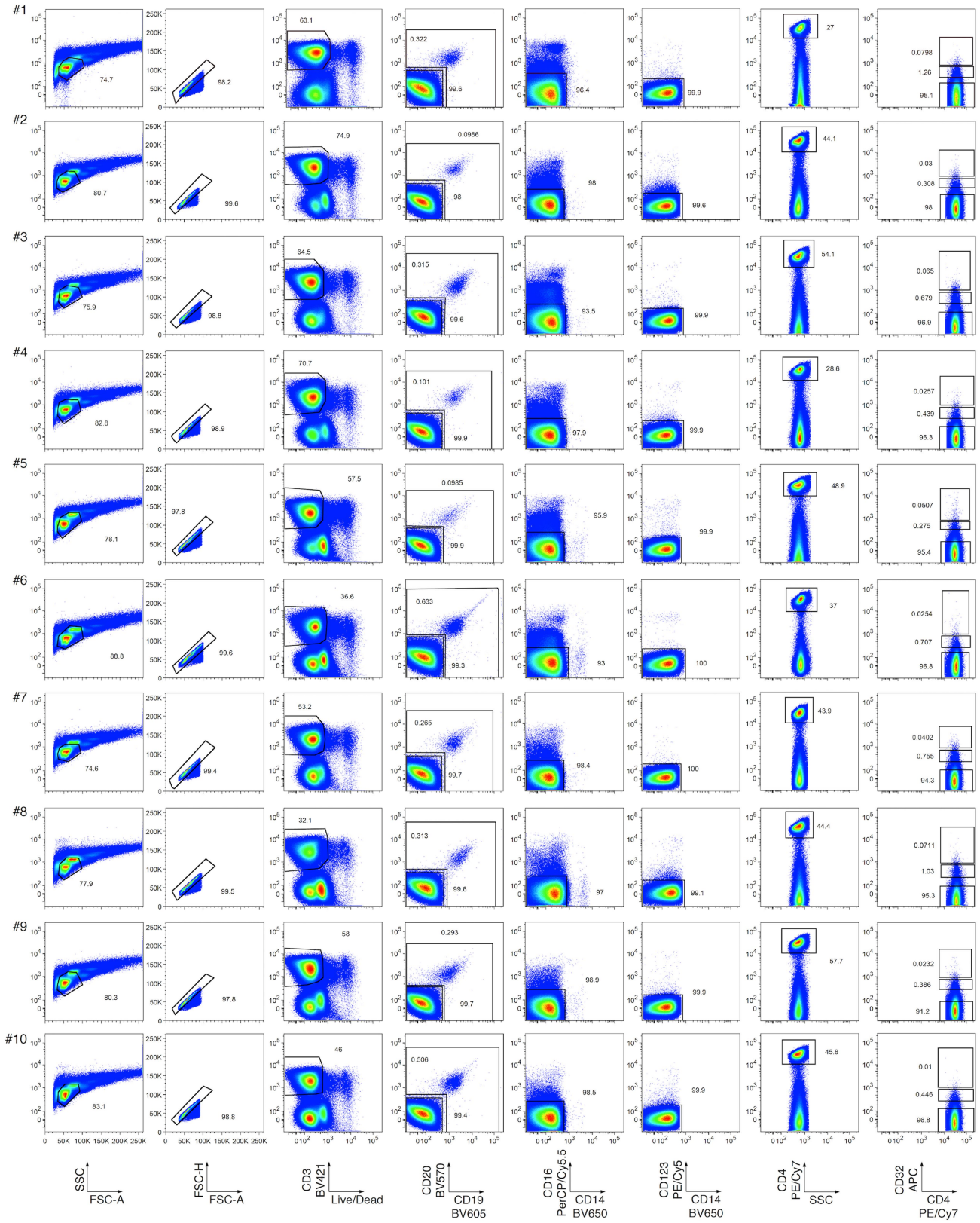

Extended Data Fig. 3 | Flow cytometry of PBMCs sorted by alternative gating for CD32^{hi}, CD32^{int} and CD32^{lo} CD4 T cell populations, as well as T cell populations bearing markers of B cells (T–B) or other non-CD4-T-cells (T–other). Cells in an inclusive light scatter gate consistent with either small lymphocytes or larger cells (first column) were enriched for single cells (second column). Within these gates, viable CD3^{+} cells (third column) that were CD19^{-} and CD20^{-} (lower gate, fourth column), CD16^{-} and CD14^{-} (fifth column), CD123^{-} (sixth column), CD4^{+} (seventh column), and CD32^{hi}, CD32^{int} or CD32^{lo} were then collected. Cells that were CD3^{+} and bearing markers of B cells (T–B; upper gate, fourth column) or other non-CD4-T-cells (T–other; combined ungated events from fifth and sixth columns) were also collected in separate tubes.

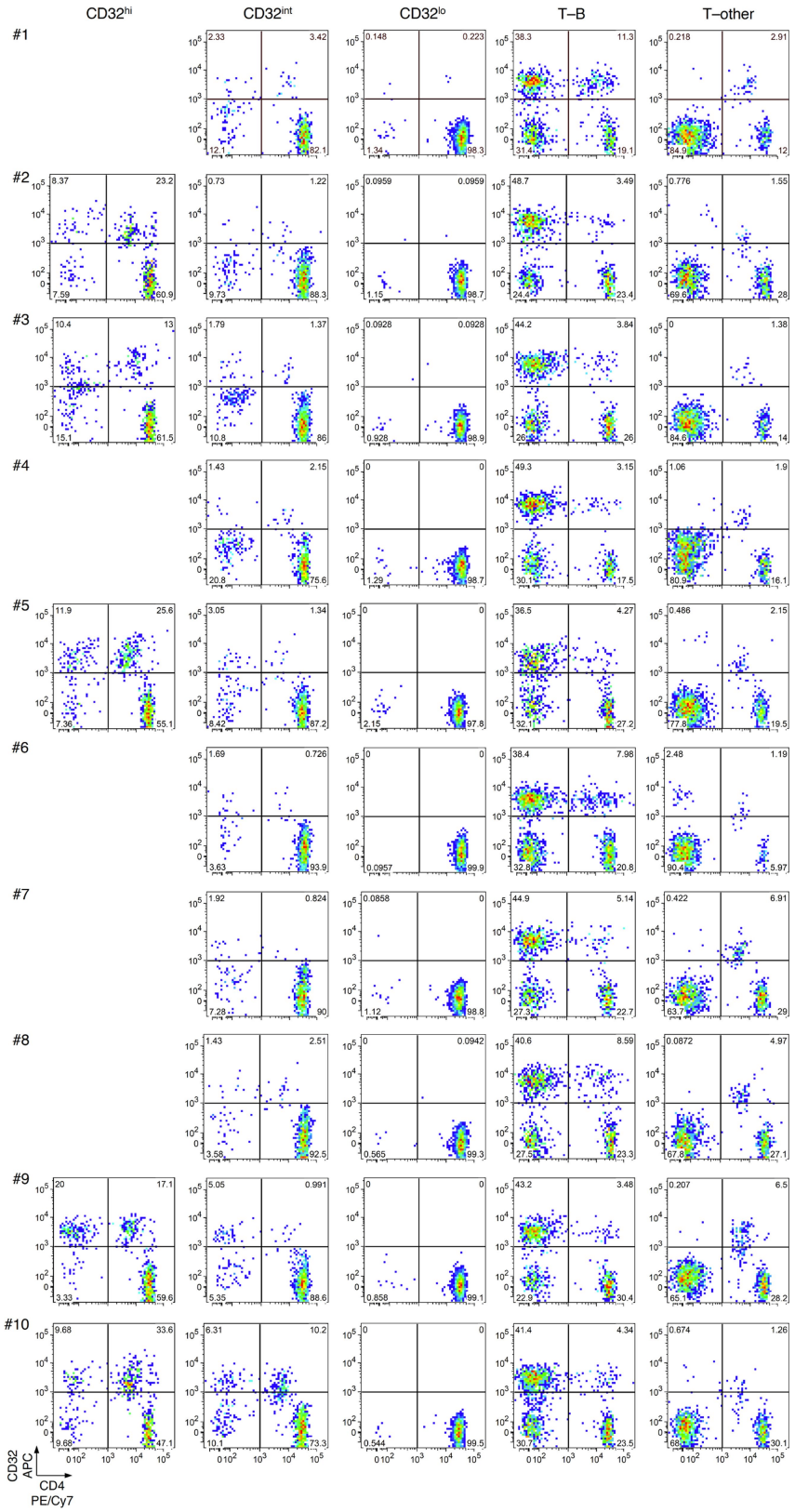

Extended Data Fig. 4 | Post-sort flow cytometry of CD32 and CD4 expression by CD32^{hi}, CD32^{int}, CD32^{lo}, T–B and T–other cell subsets. Cells were sorted as in Extended Data Fig. 3. Note the large proportions of all CD32^{+} cells that did not show high CD4 expression after sorting. Post-sort analyses of CD3^{+}CD4^{+}CD32^{hi} populations were deferred in cases in which these populations were too small to permit both post-sort analysis and downstream HIV DNA quantification (that is, donors # 1, 4 and 6–8).

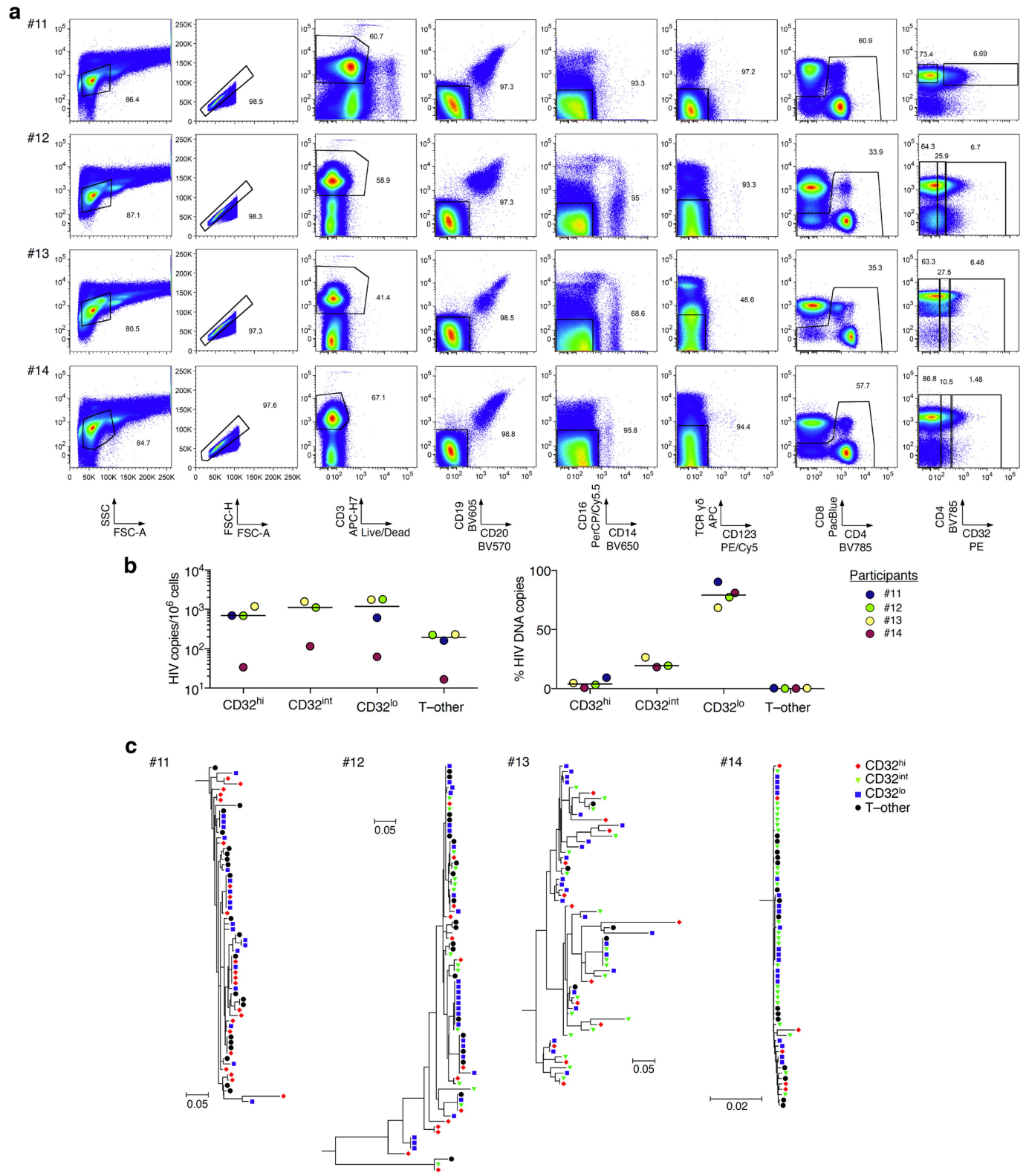

Extended Data Fig. 5 | See next page for caption.

Extended Data Fig. 5 | Flow cytometry, HIV DNA levels, and single-copy HIV DNA sequence analysis from CD32^{hi}, CD32^{int} and CD32^{lo} CD4 T cell populations, and from T cells also bearing non-CD4-T-cell markers. a, PBMCs from four additional study participants were collected from whole blood by venipuncture with immediate processing (without cryopreservation). The T–other population was collected as a combination of the ungated events from CD19/CD20, CD16/CD14 and γδ T cell receptor/CD123 exclusion plots (fourth, fifth and sixth columns). **b**, Left, copies of HIV DNA per million cells sorted from four additional study participants as in **a**. Right, percentages of all HIV DNA copies detected in blood cells deriving from CD32^{hi}, CD32^{int}, CD32^{lo} and T–other subsets, calculated by adjusting values in the left panel for the relative proportions of these subsets determined using FACS data. **c**, Sequences of individual HIV DNA copies were determined by Sanger sequencing of products obtained by fluorescence-assisted clonal amplification, which amplifies a region of the HIV *env* gene. Phylogenetic trees were constructed as described in the Supplementary Methods. All Bonferroni-corrected Slatkin–Maddison *P* values for genetic compartmentalization between any two subsets were greater than 0.05 in all four participants.

nature research

Corresponding author(s): Eli Boritz

☐ Initial submission ☐ Revised version ☒ Final submission

Life Sciences Reporting Summary

Nature Research wishes to improve the reproducibility of the work that we publish. This form is intended for publication with all accepted life science papers and provides structure for consistency and transparency in reporting. Every life science submission will use this form; some list items might not apply to an individual manuscript, but all fields must be completed for clarity.

For further information on the points included in this form, see Reporting Life Sciences Research. For further information on Nature Research policies, including our data availability policy, see Authors & Referees and the Editorial Policy Checklist.

Experimental design

1. Sample size

Describe how sample size was determined.

A group of study participants was selected to match roughly the size of the study in which the finding we wished to investigate was initially reported.

2. Data exclusions

Describe any data exclusions.

None

3. Replication

Describe whether the experimental findings were reliably reproduced.

All data acquired are reported, and so the reproducibility of the finding can be judged within the publication.

4. Randomization

Describe how samples/organisms/participants were allocated into experimental groups.

No randomization was performed.

5. Blinding

Describe whether the investigators were blinded to group allocation during data collection and/or analysis.

No blinding.

Note: all studies involving animals and/or human research participants must disclose whether blinding and randomization were used.

6. Statistical parameters

For all figures and tables that use statistical methods, confirm that the following items are present in relevant figure legends (or in the Methods section if additional space is needed).

n/a	Confirmed	
☐	☒	The exact sample size (*n*) for each experimental group/condition, given as a discrete number and unit of measurement (animals, litters, cultures, etc.)
☐	☒	A description of how samples were collected, noting whether measurements were taken from distinct samples or whether the same sample was measured repeatedly
☒	☐	A statement indicating how many times each experiment was replicated
☐	☒	The statistical test(s) used and whether they are one- or two-sided (note: only common tests should be described solely by name; more complex techniques should be described in the Methods section)
☐	☒	A description of any assumptions or corrections, such as an adjustment for multiple comparisons
☐	☒	The test results (e.g. *P* values) given as exact values whenever possible and with confidence intervals noted
☐	☒	A clear description of statistics including central tendency (e.g. median, mean) and variation (e.g. standard deviation, interquartile range)
☒	☐	Clearly defined error bars

See the web collection on statistics for biologists for further resources and guidance.

Software

Policy information about availability of computer code

7. Software

Describe the software used to analyze the data in this study.	One extended data figure legend reports negative results from Slatkin-Maddison testing for genetic compartmentalization between groups of DNA sequences. This testing was performed using HyPhy, which is deposited in GitHub. The reference for this software is included in the Supplemental Methods.

For manuscripts utilizing custom algorithms or software that are central to the paper but not yet described in the published literature, software must be made available to editors and reviewers upon request. We strongly encourage code deposition in a community repository (e.g. GitHub). *Nature Methods* guidance for providing algorithms and software for publication provides further information on this topic.

Materials and reagents

Policy information about availability of materials

8. Materials availability

Indicate whether there are restrictions on availability of unique materials or if these materials are only available for distribution by a for-profit company.	No restrictions.

9. Antibodies

Describe the antibodies used and how they were validated for use in the system under study (i.e. assay and species).	Antibodies used for flow cytometry were purchased from commercial suppliers and had been validated for use in human samples and published previously. Details of these reagents are included in the Supplemental Methods.

10. Eukaryotic cell lines

a. State the source of each eukaryotic cell line used.	None
b. Describe the method of cell line authentication used.	n/a
c. Report whether the cell lines were tested for mycoplasma contamination.	n/a
d. If any of the cell lines used are listed in the database of commonly misidentified cell lines maintained by ICLAC, provide a scientific rationale for their use.	n/a

Animals and human research participants

Policy information about studies involving animals; when reporting animal research, follow the ARRIVE guidelines

11. Description of research animals

Provide details on animals and/or animal-derived materials used in the study.	None

Policy information about studies involving human research participants

12. Description of human research participants

Describe the covariate-relevant population characteristics of the human research participants.	Human research subject participants were recruited from IRB-approval intramural NIH research protocols. All human research participants had chronic HIV infection with a history of successful treatment on antiretroviral therapy (ART).

nature research

Corresponding author(s): Eli Boritz

☐ Initial submission ☐ Revised version ☒ Final submission

Flow Cytometry Reporting Summary

Form fields will expand as needed. Please do not leave fields blank.

Data presentation

For all flow cytometry data, confirm that:

☒ 1. The axis labels state the marker and fluorochrome used (e.g. CD4-FITC).

☒ 2. The axis scales are clearly visible. Include numbers along axes only for bottom left plot of group (a 'group' is an analysis of identical markers).

☒ 3. All plots are contour plots with outliers or pseudocolor plots.

☒ 4. A numerical value for number of cells or percentage (with statistics) is provided.

Methodological details

5. Describe the sample preparation.	Peripheral blood mononuclear cells were harvested from whole peripheral blood or from leukapheresis by centrifugation over a ficoll cushion.
6. Identify the instrument used for data collection.	BD FACSAria
7. Describe the software used to collect and analyze the flow cytometry data.	FACSDiva was used for data collection. Analysis was performed in FlowJo.
8. Describe the abundance of the relevant cell populations within post-sort fractions.	Post-sort analyses of some cell populations were >98% pure, but post-sort analyses of other populations were not pure. This fact - that some sorted populations are not what they appear to be on first pass through the flow cytometer - is a key part of the argument in the manuscript.
9. Describe the gating strategy used.	All samples were initially gated using forward scatter and side scatter to identify events corresponding to cells, and then using forward scatter height vs. area to enrich for single cells. Cell populations thus gated were further gated as shown in Extended Data Figures 1, 3, and 5. The entirety of the gating for all of the samples studied is presented in the Extended Data (not in the Supplement; the ticked box below indicates that the data are included in the submission).

Tick this box to confirm that a figure exemplifying the gating strategy is provided in the Supplementary Information. ☒

The role of CD32 during HIV-1 infection

ARISING FROM B. Descours et al. *Nature* **543**, 564–567 (2017); https://doi.org/10.1038/nature21710

The persistence of latent HIV-1 in resting memory $CD4^+$ T cells is a major barrier to a cure, and a biomarker for latently infected cells would be of great scientific and clinical importance[1–5]. Using an elegant discovery-based approach, Descours et al.[6] reported that CD32a, an Fcγ receptor not normally expressed on T cells, is a potential biomarker for the HIV-1 reservoir in $CD4^+$ T cells[6]. Using a quantitative viral outgrowth assay (qVOA), we show that $CD32^+CD4^+$ T cells do not contain the majority of intact proviruses in the latent reservoir and that the enrichment found by Descours et al.[6] may in part reflect the use of an ultrasensitive ELISA that does not predict exponential viral outgrowth. Our studies show that CD32 is not a biomarker for the major population of latently infected $CD4^+$ T cells. There is a Reply to this Comment by Descours, B. et al. *Nature* **561**, https://doi.org/10.1038/s41586-018-0496-1 (2018).

If CD32a is a biomarker for latent HIV-1 infection in $CD4^+$ T cells, one that is never expressed on $CD4^+$ T cells in the absence of HIV-1 infection, then a difference in the frequency of $CD4^+$ T cells that express CD32 in HIV-1-infected individuals relative to the frequency in healthy donors is expected. We isolated $CD4^+$ T cells from infected and uninfected donors by negative selection and analysed the expression of CD32 and CD4 by flow cytometry. In healthy donors, an average of 0.019% of $CD4^+$ T cells was also $CD32^+$ (Fig. 1a). This value is not significantly different from levels in HIV-1-infected individuals (Fig. 1a; average 0.011%, $P = 0.1143$) or from values previously reported by Descours et al.[6] in HIV-1-infected individuals (0.016%, $P = 0.66$). Thus, CD32 does not seem to be a specific biomarker of latently infected $CD4^+$ T cells.

To examine whether replication-competent proviruses were present in $CD4^+CD32^{hi}$ T cells, total $CD4^+$ T cells were isolated by negative selection from six $HIV\text{-}1^+$ individuals that were treated with suppressive anti-retroviral therapy (ART) for at least 6 months (Supplementary Table 1). Freshly isolated cells were stained and sorted to obtain $CD4^+CD32^{hi}$ and $CD4^+CD32^-$ populations, which were analysed in qVOAs[7] (Fig. 1b, protocol 1). The number of $CD4^+CD32^{hi}$ cells assayed for each subject is shown in Fig. 1c. On day 14, outgrowth was measured using a standard ELISA for the HIV-1 p24 antigen. $CD4^+CD32^{hi}$ wells from all subjects were negative for p24 on day 14, and remained negative after an additional week of culture. Conversely, outgrowth was observed in $CD4^+CD32^-$ wells from all subjects on both days 14 and 21. The mean infected cell frequency, 1.37 infectious units per million cells (IUPM), was comparable to values previously measured in resting $CD4^+$ T cells in several studies (0.03–3.00 IUPM in HIV-1-infected patients[8], 0.97 IUPM in chronically infected patients[9]) and to values previously measured in the same subjects (mean value 1.33 IUPM) (Fig. 1d, Supplementary Table 2). If the enrichment of proviruses in $CD32^+$ cells reported by Descours et al.[6] was characteristic of replication-competent proviruses, then outgrowth from $CD4^+CD32^{hi}$ T cells should have been seen (Fig. 1e).

One possible explanation for the discrepancy between our results and those of Descours et al.[6] is that some latent HIV-1 may be present in a previously undescribed population of $CD4^+$ T cells that express CD32 together with other non-T-cell lineage markers. Such cells would be removed during the negative selection used to isolate $CD4^+$ T cells. Therefore, we freshly isolated total $CD4^+$ cells from infected donors on suppressive ART using two methods: negative selection to remove other lineages, leaving untouched $CD4^+$ T cells, and positive selection for cells expressing CD4 (Fig. 1b, protocol 2). Both $CD4^+$ populations were analysed by qVOA. No significant differences were observed in the frequencies of latently infected cells (Fig. 1f). Furthermore, no significant differences in proviral DNA were observed between the purified cell populations (Fig. 1g). Because CD4 is required for HIV-1 entry into the host cell, cell populations obtained via positive selection for CD4 should include every latently infected $CD4^+$ T cell. Given that neither the infected cell frequencies nor the levels of proviral DNA differed between the purified cell populations, we conclude that no additional sizable population of latently infected cells was recovered by positive CD4 selection.

In further studies, we used a cell sorting strategy identical to that of Descours et al.[6] on samples freshly isolated from six subjects receiving ART treatment. Peripheral blood mononuclear cells (PBMCs) isolated from subjects were stained and sorted to obtain $CD3^+CD4^+CD32^{hi}$ and $CD3^+CD4^+CD32^-$ cell populations that were tested for latently infected cells by qVOA analysis. The numbers of $CD3^+CD4^+CD32^{hi}$ cells assayed for each subject are shown in Fig. 1c and Supplementary Table 3. In addition, total $CD4^+$ cells were obtained by staining PBMCs for CD4 and sorting for $CD4^+$ cells (Fig. 1b, protocol 3). qVOA results showed that both the $CD3^+CD4^+CD32^-$ and the total $CD4^+$ T cell populations had the same infected cell frequencies that were comparable to frequencies measured in other studies[10]. However, we observed no outgrowth in $CD3^+CD4^+CD32^{hi}$ cultures (Fig. 1h, Supplementary Table 2).

We also analysed $CD3^+CD4^+CD32^{hi}$ and $CD3^+CD4^+CD32^-$ cells isolated by the method of Descours et al.[6] for the presence of proviral DNA by qPCR. We found 89 copies of *gag* per million $CD3^+CD4^+CD32^-$ cells, which is similar to previous measurements in total $CD4^+$ T cells[11]. However, no proviral DNA was detected after DNA extraction from 39,000 $CD3^+CD4^+CD32^{hi}$ cells and subsequent qPCR analysis (data not shown). This finding makes it highly unlikely that this cell population is enriched for HIV-1 to a level of more than one provirus copy per cell, as reported by Descours et al.[6]. We caution that the normalization of very low-level HIV-1 DNA measurements from qPCR reactions done with a low number of input cells could artificially produce apparent enrichments in HIV-1 DNA.

In a further attempt to explain the discordant qVOA results obtained in our studies and those of Descours et al.[6], we tested whether the use of the ultra-sensitive p24 digital ELISA[12] and the low cell input can affect IUPM calculations, leading to erroneous overestimation of latent infection. qVOA culture supernatants were assayed for HIV-1 p24 using the ultrasensitive SIMOA p24 2.0 assay (Quanterix) on days 5, 9, 14 and 21. Using the lower limit of quantification (0.01 pg ml^{-1}) as the cut-off level, we found that two out of three qVOAs containing $CD4^+CD32^{hi}$ cells tested positive for p24 by this assay, even though the same wells were negative by standard ELISA, which is several orders of magnitude less sensitive (Fig. 2a). Exponential outgrowth is the hallmark of replication-competent viruses. In qVOA cultures of $CD4^+CD32^-$ cells, only a fraction of the wells that were positive by SIMOA showed exponential outgrowth as determined by standard ELISA on day 21 (Fig. 2b). Importantly, $CD4^+CD32^{hi}$ culture wells that tested positive by SIMOA p24 assay showed no exponential outgrowth and had significantly lower levels of p24 (Fig. 2c). It is possible that low positive SIMOA values could reflect an assay artefact or the presence of defective proviruses that are still capable of producing low levels of Gag[13]. A further concern

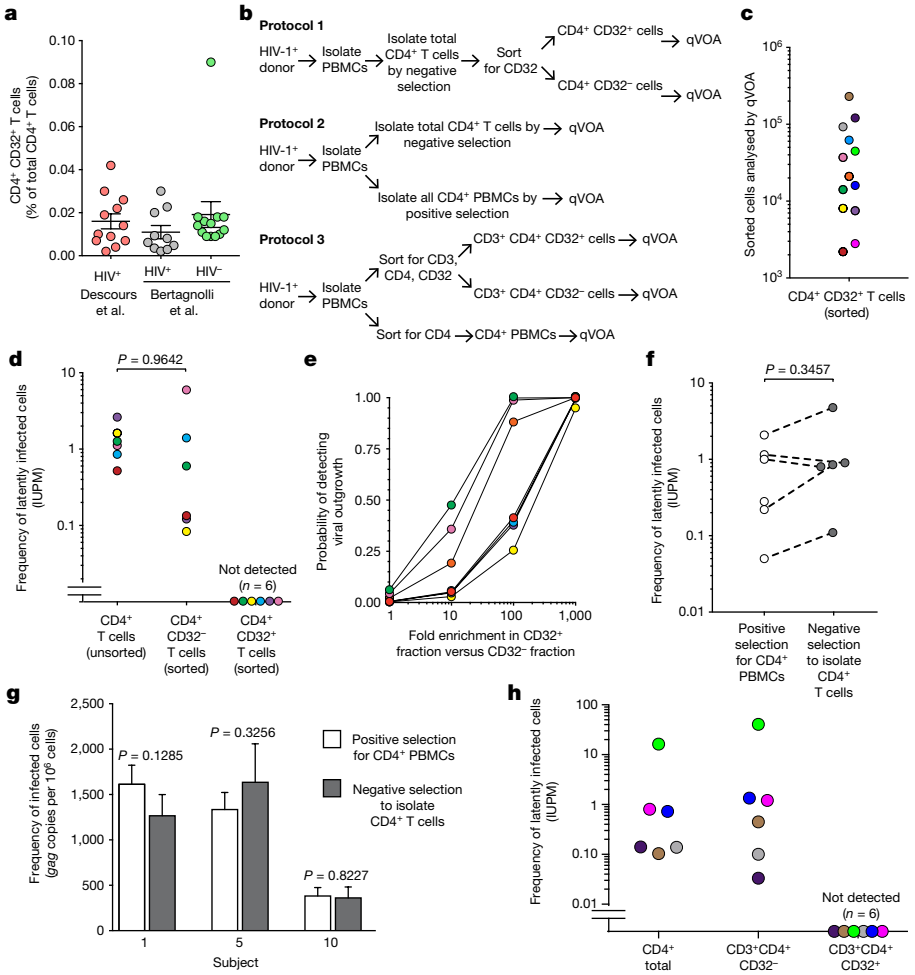

Fig. 1 | Analysis of CD4$^+$CD32$^-$ and CD4$^+$CD32$^+$ populations by qVOA and proviral DNA measurements. **a**, Percentage of CD4$^+$CD32^{hi} T cells relative to total CD4$^+$ T cells in healthy donors and HIV-1-infected donors. Infected donor values were obtained from supplementary table 4 of Descours et al.[6]. LLOQ, lower limit of quantification. **b**, Schematic depicting the three strategies (protocols 1–3) used to obtain different populations of CD4$^+$ T cells analysed in qVOAs. **c**, Numbers of sorted CD4$^+$CD32^{hi} and CD3$^+$CD4$^+$CD32^{hi} T cells from each subject analysed in qVOAs. **d**, Frequencies of latently infected cells among CD4$^+$CD32^{hi} T cells and CD4$^+$CD32$^-$ T cells and among total CD4$^+$ T cells from the same subjects previously measured in separate experiments. Cells were isolated using protocol 1 (colours correspond to subject values from panel **c**). **e**, Probability of detecting outgrowth based on measured frequencies of latently infected cells among the CD4$^+$CD32$^-$ fraction and number of CD4$^+$CD32^{hi} cells plated assuming various degrees of enrichment of HIV-1 in CD32^{hi} cells. **f**, Frequencies of latently infected cells measured in qVOAs using positive or negative selection to obtain total CD4$^+$ cells (protocol 2; positive selection was accomplished by either sorting or CD4 microbead strategies, with similar results). **g**, Comparison of proviral DNA measurements obtained with qPCR on total CD4$^+$ cells purified using positive or negative selection (protocol 2). **h**, Frequencies of latently infected cells among total CD4 cells, and CD3$^+$CD4$^+$CD32$^-$and CD3$^+$CD4$^+$CD32^{hi} populations. Cells were isolated using protocol 3 (colours correspond to subject values from panel **c**).

is that the IUPM calculations are based on cell input, fold dilutions and technical replicates[14], and thus, qVOA analyses performed with very small numbers of sorted CD4$^+$CD32^{hi} cells can markedly skew the frequency of cells harbouring replication-competent proviruses (five-fold dilutions from 800 to 1 cell in Descours et al.[6]). When we applied the results obtained with the SIMOA p24 assay, IUPM values ranged from 0 to 3,134 and 554 (patients 4 and 5, respectively; Fig. 2d). As a consequence, when we calculated the 'fold enrichment' of IUPM in the CD4$^+$CD32^{hi} cells compared to the CD4$^+$CD32$^-$ cells, we observed a mean fold enrichment of 665 (range 152–1179, from the two patients with positive p24 using SIMOA), similar to what was reported by Descours et al.[6] (Fig. 2e).

In summary, we find no evidence that CD32 expression indicates the presence of latent HIV-1, and demonstrate that at least a substantial fraction of the HIV-1 latent reservoir is in CD3$^+$CD4$^+$CD32$^-$ T cells. Although no outgrowth could be found in cultures containing CD4$^+$CD32^{hi} T cells, viral outgrowth comparable to historical measurements was found in cultures containing CD4$^+$CD32$^-$ T cells. The use of an ultrasensitive p24 ELISA assay may account for the apparent enrichment observed in culture experiments by Descours et al.[6]. In short, our results have demonstrated that CD32 does not define the HIV-1 reservoir and that future research is needed to identify biomarkers for latently infected cells.

We thank the study participants without whom this research would not be possible. Funding was provided by the US National Institutes of Health (NIH) Martin Delaney I4C, Beat-HIV and DARE Collaboratories by the Johns Hopkins Center for AIDS Research (P30AI094189), by NIH grant 43222, and by the Howard Hughes Medical Institute and the Bill and Melinda Gates Foundation.

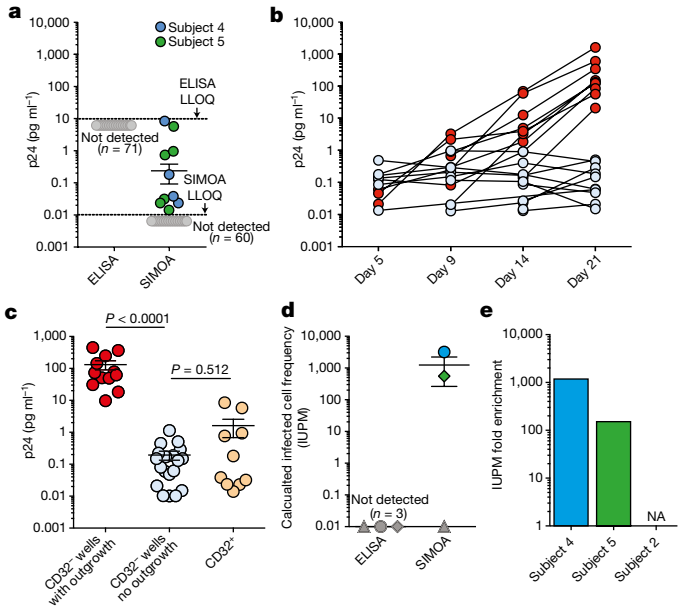

Fig. 2 | Ultrasensitive p24 measurements. a, Levels of p24 from CD32$^+$ culture wells measured by ELISA and SIMOA (lower limit of quantification: 5–10 pg ml^{-1} and 0.01 pg ml^{-1}, respectively) (data collected from three subjects, for a total of 71 wells). **b**, Longitudinal levels of p24 measured by SIMOA in individual culture wells in the qVOA for CD32$^-$ cells from subject 5, showing wells with and without viral outgrowth (red and blue circles, respectively). **c**, Levels of p24 measured by ELISA in CD32$^-$ wells with outgrowth compared with SIMOA measurements in wells with no outgrowth and CD32$^+$ wells (data collected from subjects 2, 4 and 5). *P* values were determined with a non-parametric *t*-test. **d**, IUPM calculation based on ELISA and SIMOA analysis. Symbols in dark grey represent values below the limit of detection. **e**, Fold enrichment of IUPM in CD32$^+$ cells (from subjects 2, 4 and 5). NA, not applicable.

Methods

qVOAs isolated CD4$^+$ T cells using negative depletion and were sorted for CD32$^+$ cells (Fig. 1b, protocol 1). To test whether negative depletion was causing a loss of CD32$^+$ CD4$^+$ T cells, outgrowth and proviral DNA were compared from qVOAs in which CD4$^+$ T cells were isolated using positive selection to measurements using negative depletion. Outgrowth measurements and proviral DNA were also measured using the methods described by Descours et al.[6]. Proviral DNA measurements were performed using qPCR[15]. HIV-1 p24 values were measured using both a standard ELISA for p24 antigen (Perkin Elmer) and SIMOA (Quanterix). Further details are provided in Supplementary Methods.

Data availability. All data are available from the corresponding author upon reasonable request.

Lynn N. Bertagnolli[1], Jennifer A. White[1], Francesco R. Simonetti[1], Subul A. Beg[1,2], Jun Lai[1,2], Costin Tomescu[3], Alexandra J. Murray[1], Annukka A. R. Antar[1], Hao Zhang[4], Joseph B. Margolick[4], Rebecca Hoh[5], Stephen G. Deeks[5], Pablo Tebas[6], Luis J. Montaner[3], Robert F. Siliciano[1,2]*, Gregory M. Laird[1] & Janet D. Siliciano[1]

[1]Department of Medicine, Johns Hopkins University School of Medicine, Baltimore, MD, USA. [2]Howard Hughes Medical Institute, Baltimore, MD, USA. [3]The Wistar Institute, Philadelphia, PA, USA. [4]Department of Molecular Microbiology and Immunology, Johns Hopkins Bloomberg School of Public Health, Baltimore, MD, USA. [5]Division of HIV, Infectious Diseases and Global Medicine, University of California, San Francisco, CA, USA. [6]Division of Infectious Diseases, Department of Medicine, Perelman School of Medicine at the University of Pennsylvania, Philadelphia, PA, USA. *e-mail: rsiliciano@jhmi.edu

Received: 29 September 2017; Accepted: 3 April 2018;
Published online 19 September 2018.

1. Finzi, D. et al. Identification of a reservoir for HIV-1 in patients on highly active antiretroviral therapy. *Science* **278**, 1295–1300 (1997).
2. Chun, T. W. et al. Presence of an inducible HIV-1 latent reservoir during highly active antiretroviral therapy. *Proc. Natl Acad. Sci. USA* **94**, 13193–13197 (1997).
3. Wong, J. K. et al. Recovery of replication-competent HIV despite prolonged suppression of plasma viremia. *Science* **278**, 1291–1295 (1997).
4. Richman, D. D. et al. The challenge of finding a cure for HIV infection. *Science* **323**, 1304–1307 (2009).
5. Deeks, S. G. et al. Towards an HIV cure: a global scientific strategy. *Nat. Rev. Immunol*. **12**, 607–614 (2012).
6. Descours, B. et al. CD32a is a marker of a CD4 T-cell HIV reservoir harbouring replication-competent proviruses. *Nature* **543**, 564–567 (2017).
7. Laird, G. M., Rosenbloom, D. I., Lai, J., Siliciano, R. F. & Siliciano, J. D. Measuring the frequency of latent HIV-1 in resting CD4$^+$ T cells using a limiting dilution coculture assay. *Methods Mol. Biol*. **1354**, 239–253 (2016).
8. Siliciano, J. D. et al. Long-term follow-up studies confirm the stability of the latent reservoir for HIV-1 in resting CD4$^+$ T cells. *Nat. Med*. **9**, 727–728 (2003).
9. Eriksson, S. et al. Comparative analysis of measures of viral reservoirs in HIV-1 eradication studies. *PLoS Pathog*. **9**, e1003174 (2013).
10. Crooks, A. M. et al. Precise quantitation of the latent HIV-1 reservoir: implications for eradication strategies. *J. Infect. Dis*. **212**, 1361–1365 (2015).
11. Besson, G. J. et al. HIV-1 DNA decay dynamics in blood during more than a decade of suppressive antiretroviral therapy. *Clin. Infect. Dis*. **59**, 1312–1321 (2014).
12. Passaes, C. P. & Sáez-Cirión, A. HIV cure research: advances and prospects. *Virology* **454-455**, 340–352 (2014).
13. Pollack, R. A. et al. Defective HIV-1 proviruses are expressed and can be recognized by cytotoxic T lymphocytes, which shape the proviral landscape. *Cell Host Microbe* **21**, 494-506.e4 (2017).
14. Rosenbloom, D. I. et al. Designing and interpreting limiting dilution assays: general principles and applications to the latent reservoir for human immunodeficiency virus-1. *Open Forum Infect. Dis*. **2**, ofv123 (2015).
15. Massanella, M., Gianella, S., Lada, S. M., Richman, D. D. & Strain, M. C. Quantification of total and 2-LTR (long terminal repeat) HIV DNA, HIV RNA and herpesvirus DNA in PBMCs. *Bio Protoc*. **5**, e1492 (2015).

Author contributions L.N.B., J.A.W., G.M.L., F.R.S., R.F.S. and J.D.S. designed experiments. S.A.B., C.T. and L.J.M. obtained samples. L.N.B., J.A.W., S.A.B., G.M.L., F.R.S., J.L., A.J.M., A.A.R.A. and J.D.S. performed experiments. F.R.S., H.J. and J.B.M. performed cell sorting. L.N.B., J.A.W., F.R.S., A.J.M., A.A.R.A., R.F.S. and J.D.S. analysed the data and wrote the manuscript.

Competing interests Declared none.

Additional information
Supplementary information accompanies this Comment.
Reprints and permissions information is available at http://www.nature.com/reprints.
Correspondence and requests for materials should be addressed to R.F.S.

https://doi.org/10.1038/s41586-018-0494-3

nature research

Corresponding author(s): Robert Siliciano

Life Sciences Reporting Summary

Nature Research wishes to improve the reproducibility of the work that we publish. This form is intended for publication with all accepted life science papers and provides structure for consistency and transparency in reporting. Every life science submission will use this form; some list items might not apply to an individual manuscript, but all fields must be completed for clarity.

For further information on the points included in this form, see Reporting Life Sciences Research. For further information on Nature Research policies, including our data availability policy, see Authors & Referees and the Editorial Policy Checklist.

Please do not complete any field with "not applicable" or n/a. Refer to the help text for what text to use if an item is not relevant to your study.
For final submission: please carefully check your responses for accuracy; you will not be able to make changes later.

Experimental design

1. Sample size

Describe how sample size was determined.

Sample size for the viral outgrowth experiments was increased from 6 to 12 at the request of the reviewers. In 12 of 12 patients studied by viral outgrowth assays on sorted cells, normal outgrowth was observed in populations lacking CD32+ cells and no outgrowth was found from CD32+ cells.

2. Data exclusions

Describe any data exclusions.

No data were excluded from the manuscript.

3. Replication

Describe the measures taken to verify the reproducibility of the experimental findings.

Each cell isolation protocol was repeated six times in order to ensure reproducibility.

4. Randomization

Describe how samples/organisms/participants were allocated into experimental groups.

Randomization was not relevant to this study. Participants were chosen based on having an undetectable plasma HIV- 1 RNA (< 50copies/ml) level for greater than 6 months.

5. Blinding

Describe whether the investigators were blinded to group allocation during data collection and/or analysis.

Blinding was not relevant to this study because no bias could be made by the subject or the tester in the experiments performed.

Note: all in vivo studies must report how sample size was determined and whether blinding and randomization were used.

6. Statistical parameters

For all figures and tables that use statistical methods, confirm that the following items are present in relevant figure legends (or in the Methods section if additional space is needed).

n/a	Confirmed
☐	☒ The exact sample size (*n*) for each experimental group/condition, given as a discrete number and unit of measurement (animals, litters, cultures, etc.)
☐	☒ A description of how samples were collected, noting whether measurements were taken from distinct samples or whether the same sample was measured repeatedly
☐	☒ A statement indicating how many times each experiment was replicated
☐	☒ The statistical test(s) used and whether they are one- or two-sided *Only common tests should be described solely by name; describe more complex techniques in the Methods section.*
☒	☐ A description of any assumptions or corrections, such as an adjustment for multiple comparisons
☐	☒ Test values indicating whether an effect is present *Provide confidence intervals or give results of significance tests (e.g. P values) as exact values whenever appropriate and with effect sizes noted.*
☐	☒ A clear description of statistics including central tendency (e.g. median, mean) and variation (e.g. standard deviation, interquartile range)
☐	☒ Clearly defined error bars in all relevant figure captions (with explicit mention of central tendency and variation)

See the web collection on statistics for biologists for further resources and guidance.

Software

Policy information about availability of computer code

7. Software

Describe the software used to analyze the data in this study.	Infectious units per million were calculated using the infection frequency calculator, which can be found at: http://silicianolab.johnshopkins.edu.

For manuscripts utilizing custom algorithms or software that are central to the paper but not yet described in the published literature, software must be made available to editors and reviewers upon request. We strongly encourage code deposition in a community repository (e.g. GitHub). *Nature Methods* guidance for providing algorithms and software for publication provides further information on this topic.

Materials and reagents

Policy information about availability of materials

8. Materials availability

Indicate whether there are restrictions on availability of unique materials or if these materials are only available for distribution by a third party.	No unique material was used and all materials can be obtained from a standard commercial source.

9. Antibodies

Describe the antibodies used and how they were validated for use in the system under study (i.e. assay and species).	For the flow cytometry and sorting included in this paper, the antibodies that were used include: APC-CD32 (Biolegend; FUN-2 Clone; Catalog # 303208), FITC-CD32 (Biolegend; FUN-2 Clone; Catalog # 303204), APC-CD4 (BD Pharmingen; RPA-T4 clone; Catalog # 564975), PE-CD4 (BD Pharmingen; RPA-T4 clone; Catalog # 561844), and BV421-CD3 (BD Pharmingen; UCHT1 clone; Catalog # 562426).

10. Eukaryotic cell lines

a. State the source of each eukaryotic cell line used.	MOLT4/CCR5 cell line was obtained from the AIDS Reagent Bank.
b. Describe the method of cell line authentication used.	The cell line used in the quantitative viral outgrowth assay was validated by Laird et. al., PLoS Pathogens 2013.
c. Report whether the cell lines were tested for mycoplasma contamination.	The MOLT4/CCR5 cell line was negative for mycoplasma contamination.
d. If any of the cell lines used are listed in the database of commonly misidentified cell lines maintained by ICLAC, provide a scientific rationale for their use.	No commonly misidentified cells lines were used.

Animals and human research participants

Policy information about studies involving animals; when reporting animal research, follow the ARRIVE guidelines

11. Description of research animals

Provide all relevant details on animals and/or animal-derived materials used in the study.	No animals were used.

Policy information about studies involving human research participants

12. Description of human research participants

Describe the covariate-relevant population characteristics of the human research participants.	All HIV-1 infected research participants that were included in this study had undetectable plasma HIV- 1 RNA (< 50copies/ml) for greater than 6 months.

nature research

Corresponding author(s): Robert Siliciano

Flow Cytometry Reporting Summary

Form fields will expand as needed. Please do not leave fields blank.

Data presentation

For all flow cytometry data, confirm that:

☒ 1. The axis labels state the marker and fluorochrome used (e.g. CD4-FITC).

☒ 2. The axis scales are clearly visible. Include numbers along axes only for bottom left plot of group (a 'group' is an analysis of identical markers).

☒ 3. All plots are contour plots with outliers or pseudocolor plots.

☒ 4. A numerical value for number of cells or percentage (with statistics) is provided.

Methodological details

5. Describe the sample preparation.	Peripheral blood mononuclear cells (PBMCs) were isolated from whole blood using density centrifugation on a Ficoll-Hypaque gradient.
6. Identify the instrument used for data collection.	Flow cytometry for healthy donor and HIV-infected donor CD32 frequency analysis was performed using the iQue Screener Plus (Intellicyt Corporation). Cell populations used in quantitative viral outgrowth assays were sorted using either a SH800 cell sorter (Sony Biotechnology) or a Beckman Coulter MoFlo Cell Sorter.
7. Describe the software used to collect and analyze the flow cytometry data.	Sort data was analyzed using the Summit software version 4.3 from Beckman Coulter.
8. Describe the abundance of the relevant cell populations within post-sort fractions.	Purity was determined by running a purity check of the sorted populations after the sort was completed. CD32- fractions had a purity of greater than 98% for each sort that was completed.
9. Describe the gating strategy used.	Preliminary gates were set to collect viable lymphocytes and singlets. Then the specific sorted population gates were based on the isotype controls.

Tick this box to confirm that a figure exemplifying the gating strategy is provided in the Supplementary Information. ☒

Corrected: Publisher Correction

Evidence that CD32a does not mark the HIV-1 latent reservoir

ARISING FROM B. Descours et al. *Nature* **543**, 564–567 (2017); https://doi.org/10.1038/nature21710

A recent report by Descours et al.[1] suggests that the cell surface expression of the low affinity Fc receptor CD32a (also known as FcγRIIa) marks the replication-competent HIV-1 reservoir in CD4$^+$ T cells from 12 HIV-1-infected participants receiving suppressive anti-retroviral therapy (ART)[1]. We have undertaken considerable efforts to replicate these findings using peripheral blood mononuclear cells (PBMCs) from 20 HIV-1-infected, ART-suppressed participants (Extended Data Table 1). We found no evidence to suggest that CD32a marks a CD4$^+$ T cell population enriched in either HIV-1 DNA or replication-competent HIV-1 in our study participants. There is a Reply to this Comment by Descours, B. et al. *Nature* **561**, https://doi.org/10.1038/s41586-s41586-018-0496-1 (2018).

To validate these findings, we adopted the same gating strategy as described by Descours et al.[1] to define CD4$^+$ T cell populations (Supplementary Fig. 1a). The CD32 antigen was identified using the same antibody clone (FUN-2) as described by Descours et al.[1]. We observed the same CD4$^+$ T cell subsets that stained at a high cell surface density of CD32 (CD4$^+$CD32^{high}), an intermediate cell surface density of CD32 (CD4$^+$CD32^{int}), and a CD4$^+$ T cell subset lacking CD32 expression (CD4$^+$CD32^{neg}). We obtained frequencies of CD4$^+$CD32^{high} T cells that ranged from 0.002% to 0.026%, with a median value (0.012%) that was identical to that reported by Descours et al.[1] (Extended Data Table 2 and Supplementary Fig. 1a). Notably, we confirmed that this same CD4$^+$CD32^{high} population is also present in PBMCs isolated from eight healthy donors and exists at similar frequencies to that in HIV-1-infected samples ($P = 0.971$, Extended Data Fig. 1a).

Next, we assessed the amount of replication-competent HIV-1 isolated from the same 20 participants by measuring the infectious unit per million cells (IUPM) in CD4$^+$ T cells (range 0.01–37.5, median 0.46). Participant CD4$^+$CD32^{high} T cell populations were colour-coded in descending order, and then divided into quartiles that corresponded to the relative frequency of CD4$^+$CD32^{high} cells present in these samples (Fig. 1a).

After cytometric sorting of the various CD4$^+$CD32 subsets, we quantified HIV-1 DNA in each population (total CD4$^+$, CD4$^+$CD32^{neg}, CD4$^+$CD32^{int} and CD4$^+$CD32^{high}, Fig. 1b) using droplet digital PCR (ddPCR), as described in the Methods. We found no evidence of HIV-1 DNA enrichment in the CD4$^+$CD32^{high} fraction. We observed no significant difference in HIV-1 DNA between any populations and the CD4$^+$CD32^{high} T cell population ($P = 0.28$). In fact, levels of HIV-1 DNA in the CD4$^+$CD32^{high} T cell subsets isolated from nine participants was at the assay limit of detection (Fig. 1b). After correction for cell input in the CD4$^+$CD32^{high} fraction, as estimated DNA values, we saw no evidence for HIV-1 DNA enrichment (open symbols in Extended Data Fig. 1b).

We then compared the relative frequency of the CD4$^+$CD32^{high} T cell populations and the viral replicative capacity (IUPM values) per participant, but no relationship between the two parameters was observed (Fig. 1c). All values have been tabulated in Extended Data Table 2.

The HIV-1 reservoir largely resides in quiescent CD4$^+$ T cells[2,3]. Therefore, we sought to confirm the activation status of the CD4$^+$ T cell populations by measuring the frequency of the activation markers CD69, CD25 and HLA-DR on CD4$^+$ T cell subsets from all participants. We found that the CD4$^+$CD32^{high} T cells were highly activated compared to the CD4$^+$CD32^{neg} T cells ($P < 0.0001$). Notably, among the activation markers, HLA-DR was particularly enriched,

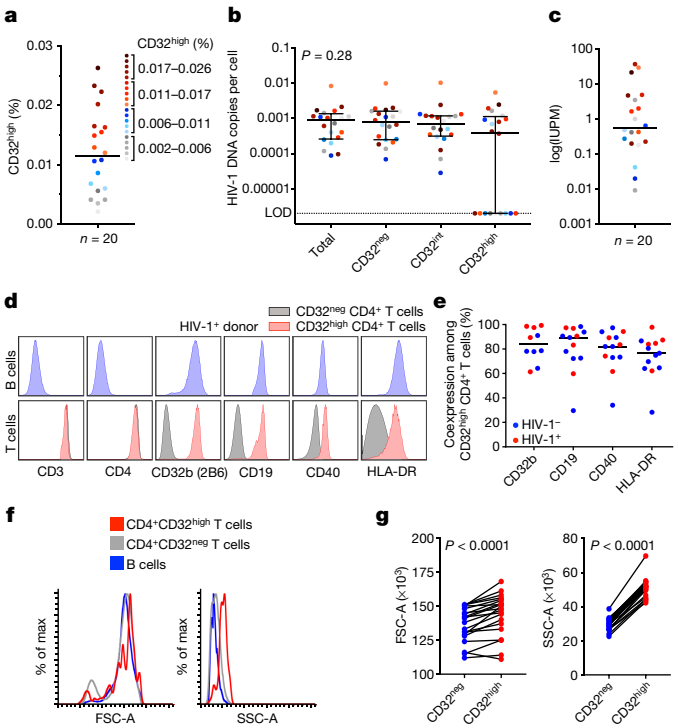

Fig. 1 | CD32-expressing CD4$^+$ T cells are not enriched in HIV-1 DNA and express markers of B cell origin. a–c, CD4$^+$CD32^{int} and CD4$^+$CD32^{high} T cells from PBMCs of ART-suppressed, HIV-1-infected patients ($n = 20$) were sorted, and HIV-1 DNA was measured by ddPCR. **a**, Dividing the frequency (in percentage) of CD4$^+$CD32^{high} T cells from all participants into quartiles, the values are shown as below or above the median. **b**, DNA copies per cell in sorted subsets of total CD4$^+$, CD4$^+$CD32^{neg}, CD4$^+$CD32^{int} and CD4$^+$CD32^{high} T cells are shown, with median and interquartile range (IQR). *P* value determined by Kruskal–Wallis test. LOD, limit of detection. **c**, IUPM in CD4$^+$ T cells of each participant is shown in the colour corresponding to its frequency of CD4$^+$CD32^{high} cells in panel **a**. **d**, **e**, CD32^{neg} and CD32^{high} (identified using FUN-2) CD4$^+$ T cells from human PBMCs were assessed by flow cytometry for the expression of CD32b (2B6 antibody), CD19, CD40 and HLA-DR and compared to B cells (CD3$^-$CD14$^-$CD19$^+$ lymphocytes). **d**, Representative flow cytometry results per cell antigen levels on B cells (top, blue histograms) and on CD32^{neg} and CD32^{high} CD4$^+$ T cells (bottom, grey and red histograms, respectively) from PBMCs from an HIV-1$^+$ participant. **e**, Frequency of CD4$^+$CD32^{high} T cells staining positive for CD32b (2B6), CD19, CD40 or HLA-DR from HIV-1$^+$ ($n = 5$) and HIV-1$^-$ ($n = 5$–8) human donor PBMC samples. Bars denote median values. **f**, Representative histograms of the FSC-A and SSC-A of B cells and CD32^{neg} and CD32^{high} CD4$^+$ T cells from PBMCs of an HIV-1$^+$, ART-suppressed participant sorted on a BD FACSAria II. **g**, Comparisons of the median FSC-A and SSC-A values between CD32^{neg} and CD32^{high} CD4$^+$ T cell subsets from HIV-1$^+$, ART-suppressed participants ($n = 20$). *P* values were determined using a paired *t*-test.

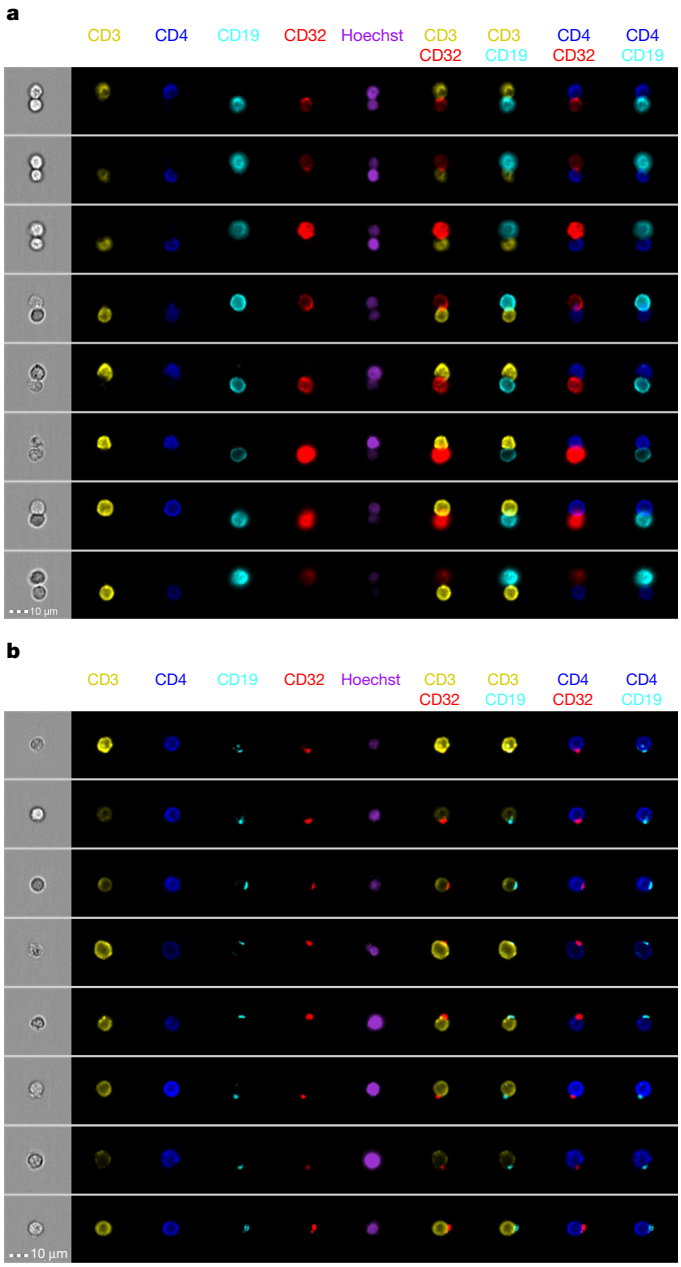

Fig. 2 | Flow cytometry imaging of sorted CD32-expressing T cells. **a**, Representative bright-field and pseudo-colour fluorescence images of T–B cell conjugates found in the CD32^{high} CD4^{+} T cell population sorted from PBMCs from HIV-1^{+}, ART-suppressed participants, and imaged using Amnis technology. **b**, Representative images of punctate CD32 staining found on single T cells in the CD32^{high} and CD32^{int} population sorted from HIV-1^{+}, ART-suppressed participant PBMCs.

marking approximately 75% of all CD4^{+}CD32^{high} cells (median 74%), compared to CD4^{+}CD32^{neg} cell populations (median 1.4%) (Extended Data Fig. 1c, $P < 0.0001$).

Two CD32 isoforms (CD32a and CD32b) are known to be expressed among all antigen presenting cells (APCs), but not typically on T cells. Therefore, we sought to exclude any APCs as potential contaminants of flow cytometry sorting. We evaluated the co-expression of lineage markers for all major CD32-bearing cells including monocytes, B cells, dendritic cells, granulocytes and natural killer cells. As expected, all CD32^{+} T cells expressed high amounts of CD3 and CD4 (Fig. 1d). However, we found that most CD4^{+}CD32^{high} T cells from HIV-1^{+} patients, and also from healthy donors, co-expressed several B cell markers including CD19, CD40 and HLA-DR (Fig. 1d, e, Extended Data Fig. 2a). Notably, the B cell antigens found on CD4^{+}CD32^{high} T cells were present at similar cell-surface densities as detected on bona fide B cells (Fig. 1d, e, Extended Data Fig. 2a).

The demonstration that the CD4^{+}CD32^{high} fraction seen in HIV-1^{+} patients was marked with several B cell antigens and was similarly present in naive donors led us to investigate the origin of these B cell markers on a CD4^{+} T cell. Several reports have shown that B cells exclusively express the CD32b isoform[4]. The FUN-2 antibody clone used by Descours et al.[1] cannot distinguish between the CD32a and CD32b isoforms. Therefore, we used the monoclonal antibody clone 2B6 that has been reported to exclusively bind to CD32b[4,5]. After co-staining PBMCs from HIV-1^{+} and HIV-1^{-} individuals with both the FUN-2 and the 2B6 antibodies, we found that all CD4^{+}CD32^{high} T cells were marked only by the CD32b isoform and not by CD32a (Fig. 1d, e, Extended Data Fig. 2b), indicating that B cells are the origin of the CD32b antigen that marks the CD4^{+}CD32^{high} T cells.

We sought to confirm this by determining whether *CD32A* (also known as *FCGR2A*) or *CD32B* (*FCGR2B*) mRNA was endogenously produced in the CD4^{+}CD32^{high} subsets. After isolating total cellular RNA from various sorted T cell subsets, we used established reverse transcription PCR (RT–PCR) primers and probes that are specific to the CD32a and CD32b isoforms, as described in the Methods. We found that sorted CD4^{+}CD32^{high} T cells from four HIV-1-infected participants did not contain detectable levels of the *CD32A* isoform. However, the *CD32B* mRNA isoform was readily detected in CD4^{+}CD32^{high} T cells isolated from two out of four HIV-1^{+} patients (Extended Data Fig. 2c). By additional RT–PCR analysis, we detected both *CD3G* and *CD19* transcripts in the same CD4^{+}CD32^{high} T population, indicating that the CD32b marking the CD4^{+}CD32^{high} T cells may be from B cells expressing cognate CD32b (Extended Data Fig. 2d).

Because this may require cell-to-cell interaction, we performed a back-gating analysis of our flow cytometry data and confirmed that all CD4^{+}CD32^{high} populations were identified within single-cell gates (Supplementary Fig. 1b). However, post-hoc analysis comparing the forward and side scatter light pulse area (FSC-A and SSC-A, respectively) values between CD4^{+}CD32^{neg} and CD4^{+}CD32^{high} T cells showed that the CD4^{+}CD32^{high} populations had both a significantly higher FSC-A ($P < 0.0001$) and SSC-A ($P < 0.0001$), suggesting that the CD4^{+}CD32^{high} population may consist largely of cell doublets (Fig. 1f, g).

We next used Amnis imaging flow cytometry to visualize the sorted CD4^{+}CD32^{neg}, CD4^{+}CD32^{int} and CD4^{+}CD32^{high} cell populations directly. As expected, the CD4^{+}CD32^{neg} and the CD4^{+}CD32^{int} cell populations each consisted of more than 99% single cells. However, the CD4^{+}CD32^{high} fraction contained a high frequency of cell doublets (mean value 94%) (Extended Data Fig. 3). Of these 'doublets', approximately 70% seemed to be coincident doublets, and 30% were conjugates of T and B cells (Fig. 2a and Extended Data Fig. 3b).

We observed no examples in which CD32 staining on T cells was distributed throughout the cell membrane, supporting the idea that the CD32 found in the CD4^{+}CD32^{high} population is not the result of endogenous expression from CD4^{+} T cells. Of the instances in which CD32 was detected on a T cell in the CD4^{+}CD32^{high} population, the staining was punctate and often co-localized with punctate CD19 staining (Fig. 2b), suggesting that CD32 was acquired via contact between B and T cells. We noted that the frequency of T cells with punctate CD32 staining was substantially higher in the sorted CD32^{int} population. Thus, sorting for CD4^{+} T cells with a 'high' surface density of CD32 results in the selective enrichment of contaminating T–B cell doublets. As shown in Supplementary Fig. 1, these doublets cannot be discerned by routine cytometric FSC and SSC singlet gating strategies.

In summary, using samples from 20 HIV-1-infected, ART-suppressed participants, our data contradict the assertion that CD32a is a marker of

the replication-competent viral reservoir. Although we did detect similar frequencies of $CD4^+CD32^{high}$ populations to Descours et al.[1], we found no difference in the total HIV-1 DNA content between $CD4^+$ T cell populations including or excluding the $CD32^{high}$ fractions (Fig. 1b).

Notably, the $CD4^+CD32^{high}$ population was highly activated. Previous studies that have evaluated CD32 expression on T cells suggest that it may be detected after activation[6,7] and led us to believe that this population may be atypical compared to a quiescent population harbouring the HIV-1 reservoir[2,3].

Our additional findings are incongruent with CD32a marking the replication-competent reservoir in $CD4^+$ T cells; our phenotyping and RT–PCR experiments indicate that it is the CD32b isoform that marks the $CD4^+CD32^{high}$ cells (Fig. 1d, e, Extended Data Fig. 2b–d). This finding, combined with the demonstration that this cell population is found in uninfected individuals, conflicts with the assertion of Descours et al.[1] that CD32a is upregulated after the establishment of viral latency. Recent reports have corroborated the absence of CD32a transcripts in reactivated, clonal HIV-1-infected $CD4^+$ T cells[8].

The surface density of CD32b (and other B cell markers) on the $CD4^+CD32^{high}$ population was observed at similar densities to that on B cells. These data, combined with the post-hoc analysis, suggests that this population may be largely comprised of doublets. Direct interrogation of the $CD4^+CD32^{high}$ population via Amnis imaging confirmed that this population consisted largely of contaminating doublets; either co-incident events or cell-to-cell conjugates (Fig. 2a).

We demonstrate that the mechanism by which the CD32b isoform labels the $CD4^+CD32^{high}$ populations is through the direct interaction of $CD4^+$ T and B cells, and possible trogocytotic transfer of B cell antigens to T cells, as observed in the $CD4^+CD32^{int}$ population (Fig. 2b). This may explain the transfer or membrane painting of antigens such as CD32b, CD40 and HLA-DR, among other markers[9–11]. Not only have cell-to-cell membrane transfers been shown to occur commonly in vivo during viral infections, but such transfers largely occur on activated cells[12]. Membrane-bound Fcγ receptors, including CD32b, are known to be extracted from APCs and then transferred to T cells, and serve as a surrogate of recent T cell and APC interactions[13]. Our demonstration of T–B cell conjugates in the $CD4^+CD32^{high}$ population and high levels of single cells in the $CD4^+CD32^{int}$ population support this notion (Fig. 2a, b).

Collectively, our findings confirm that selectively sorting for T cells with a high surface density of CD32 results in the enrichment of T–B cell doublet contaminants, which cannot be discerned by routine gating strategies. The true isoform, CD32b, that marks the $CD4^+CD32^{high}$ population is probably indicative of dynamic $CD4^+$ T cell interaction with B cells, rather than a marker of the HIV-1 reservoir[14,15].

We thank S. Mordecai for Amnis technical expertise, and acknowledge support from NIAID grants AI091514, AI122942, AI127089 and AI131365 awarded to J.B.W. Support was also provided by the NIAID awarded Martin Delaney Collaboratory 'BELIEVE' grant AI126617, co-funded by NIDA, NIMH and NINDS awarded to D.F.N.

Methods

HIV-1^+ participants were recruited through: The Maple Leaf Medical clinic in Toronto, Canada; The HIV Eradication and Latency (HEAL) cohort of Brigham and Women's and Massachusetts General Hospital; The Whitmann Walker Clinic in Washington, DC; or the Hospital of the University of Pennsylvania. The study was approved by the University of Toronto, The University of Pennsylvania and George Washington University ethics committees and according to the protocol approved by the Partners Human Research Committee and Institutional Review Board (IRB). Written informed consent was obtained from each participant.

The percentage of $CD32^+$ (clone FUN-2) $CD4^+$ T cells was measured in samples from study participants. Both $CD32^+$ and $CD32^{neg}$ $CD4^+$ T cells were sorted and viral DNA was measured using ddPCR. The analysis of cell lineage markers by flow cytometry and RT–PCR was also conducted. Flow cytometry sorts from PBMCs used in HIV-1 DNA analyses were performed on cell subsets and assessed using Amnis imaging flow cytometry.

Data availability. All data and reagents are available from the corresponding author upon request.

Christa E. Osuna[1,7], So-Yon Lim[1,7], Jessica L. Kublin[1,7], Richard Apps[2], Elsa Chen[1], Talia M. Mota[3], Szu-Han Huang[3], Yanqin Ren[3], Nathaniel D. Bachtel[3], Athe M. Tsibris[4], Margaret E. Ackerman[5], R. Brad Jones[3], Douglas F. Nixon[3] & James B. Whitney[1,6]*

[1]Center for Virology and Vaccine Research, Beth Israel Deaconess Medical Center, Harvard Medical School, Boston, MA, USA. [2]Center for Human Immunology, National Institute of Allergy and Infectious Diseases, Bethesda, MD, USA. [3]Division of Infectious Diseases, Weill Department of Medicine, Weill Cornell Medical College, New York, NY, USA. [4]Brigham and Women's Hospital, Boston, Massachusetts Harvard Medical School, Boston, MA, USA. [5]Thayer School of Engineering, Dartmouth College, Hanover, NH, USA. [6]Ragon Institute of MGH, MIT, and Harvard, Cambridge, MA, USA. [7]These authors contributed equally: Christa E. Osuna, So-Yon Lim, Jessica L. Kublin. *e-mail: jwhitne2@bidmc.harvard.edu

Received: 11 August 2017; Accepted: 24 May 2018;
Published online 19 September 2018.

1. Descours, B. et al. CD32a is a marker of a CD4 T-cell HIV reservoir harbouring replication-competent proviruses. *Nature* **543**, 564–567 (2017).
2. Chun, T. W. et al. Quantification of latent tissue reservoirs and total body viral load in HIV-1 infection. *Nature* **387**, 183–188 (1997).
3. Finzi, D. et al. Identification of a reservoir for HIV-1 in patients on highly active antiretroviral therapy. *Science* **278**, 1295–1300 (1997).
4. Veri, M. C. et al. Monoclonal antibodies capable of discriminating the human inhibitory Fcγ-receptor IIB (CD32B) from the activating Fcγ-receptor IIA (CD32A): biochemical, biological and functional characterization. *Immunology* **121**, 392–404 (2007).
5. Boruchov, A. M. et al. Activating and inhibitory IgG Fc receptors on human DCs mediate opposing functions. *J. Clin. Invest.* **115**, 2914–2923 (2005).
6. Engelhardt, W., Matzke, J. & Schmidt, R. E. Activation-dependent expression of low affinity IgG receptors FcγRII(CD32) and FcγRIII(CD16) in subpopulations of human T lymphocytes. *Immunobiology* **192**, 297–320 (1995).
7. Sandilands, G. P. et al. Differential expression of CD32 isoforms following alloactivation of human T cells. *Immunology* **91**, 204–211 (1997).
8. Cohn, L. B. et al. Clonal $CD4^+$ T cells in the HIV-1 latent reservoir display a distinct gene profile upon reactivation. *Nat. Med.* **24**, 604–609 (2018).
9. Cone, R. E., Sprent, J. & Marchalonis, J. J. Antigen-binding specificity of isolated cell-surface immunoglobulin from thymus cells activated to histocompatibility antigens. *Proc. Natl Acad. Sci. USA* **69**, 2556–2560 (1972).
10. Hwang, I. et al. T cells can use either T cell receptor or CD28 receptors to absorb and internalize cell surface molecules derived from antigen-presenting cells. *J. Exp. Med.* **191**, 1137–1148 (2000).
11. Wetzel, S. A., McKeithan, T. W. & Parker, D. C. Peptide-specific intercellular transfer of MHC class II to CD4+ T cells directly from the immunological synapse upon cellular dissociation. *J. Immunol.* **174**, 80–89 (2005).
12. Rosenits, K., Keppler, S. J., Vucikuja, S. & Aichele, P. T cells acquire cell surface determinants of APC via *in vivo* trogocytosis during viral infections. *Eur. J. Immunol.* **40**, 3450–3457 (2010).
13. Daubeuf, S. et al. Preferential transfer of certain plasma membrane proteins onto T and B cells by trogocytosis. *PLoS One* **5**, e8716 (2010).
14. Garside, P. et al. Visualization of specific B and T lymphocyte interactions in the lymph node. *Science* **281**, 96–99 (1998).
15. Okada, T. et al. Antigen-engaged B cells undergo chemotaxis toward the T zone and form motile conjugates with helper T cells. *PLoS Biol.* **3**, e150 (2005).

Author contributions D.F.N. and J.B.W. designed the studies. R.B.J., R.A., E.C., Y.R., N.D.B., C.E.O., R.T. and S.Y.L. led the virology assays. S.H.H., D.C., J.L.K., M.A. and C.E.O. led the immunology assays. J.B.W. led the studies and wrote the paper with all co-authors.

Competing interests Declared none.

Additional information
Extended data accompanies this Comment.
Supplementary information accompanies this Comment.
Reprints and permissions information is available at http://www.nature.com/reprints.
Correspondence and requests for materials should be addressed to J.B.W.

https://doi.org/10.1038/s41586-018-0495-2

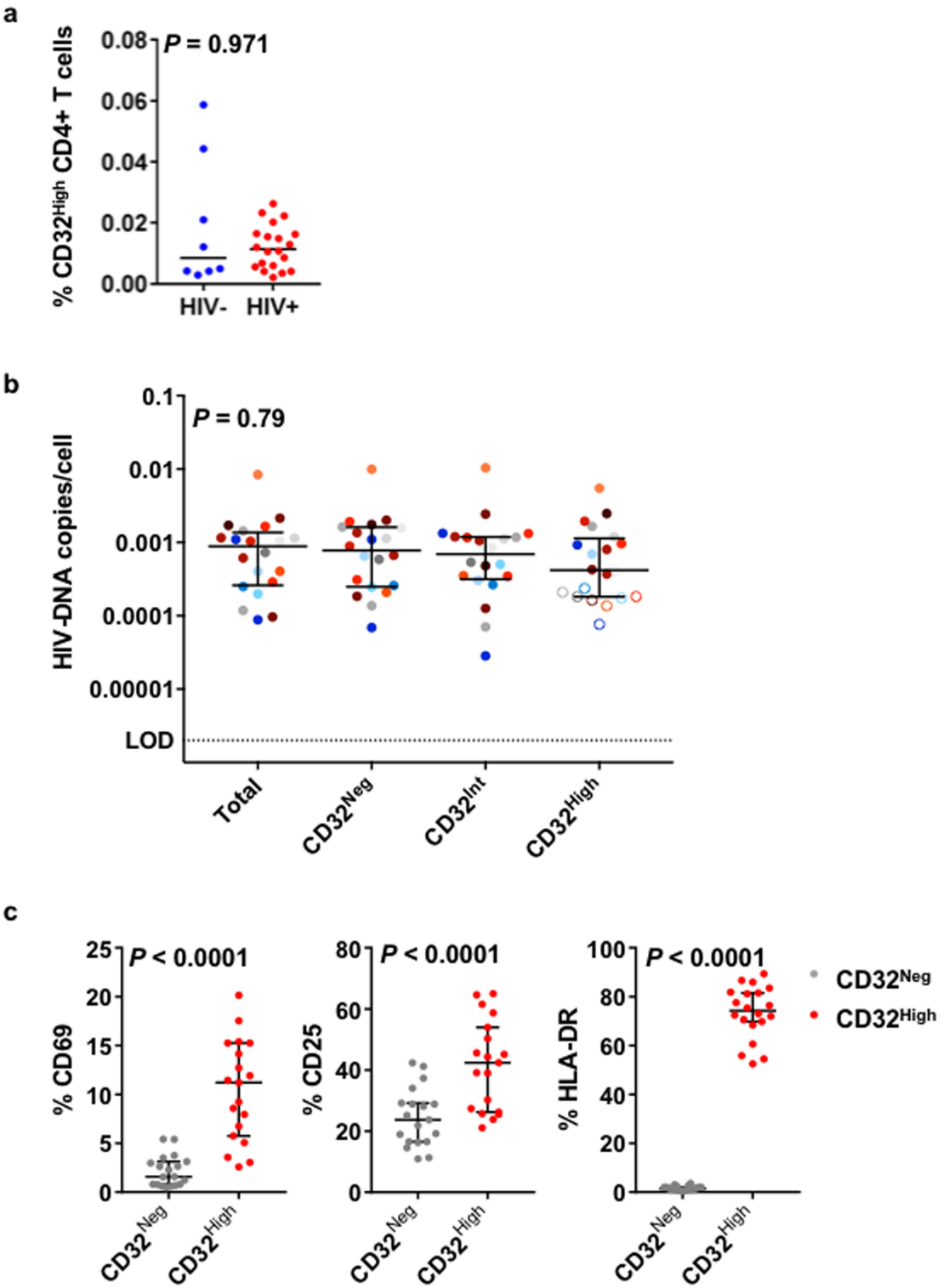

Extended Data Fig. 1 | Frequency and activation status of CD32-expressing CD4$^+$ T cells and their HIV-1 DNA content. a, The frequency of CD32^{high} CD4$^+$ T cells was measured by flow cytometry in PBMCs from ART-suppressed, HIV-1$^+$ ($n = 20$) and HIV-1$^-$ ($n = 8$) donors. Bars denote median values. *P* values were determined by a Mann–Whitney test. **b**, DNA copies per cell in sorted subsets of total CD4$^+$, CD4$^+$CD32^{neg}, CD4$^+$CD32^{int} and CD4$^+$CD32^{high} T cells are shown with median values and the IQR. The results are shown as either the actual HIV-1 DNA copies per million cells (filled symbols) or as estimated values calculated using the LOD and applied to the number of cells when the DNA input did not reach the threshold (open symbols). *P* values were determined by a Kruskal–Wallis test. **c**, The percentage of CD69, CD25 and HLA-DR expression was measured by flow cytometry on CD32^{neg} and CD32^{high} (FUN-2) CD4$^+$ T cells from PBMCs from HIV-1$^+$ participants ($n = 20$). Error bars show the median and IQR. *P* values were determined by Wilcoxon matched-pairs signed rank tests.

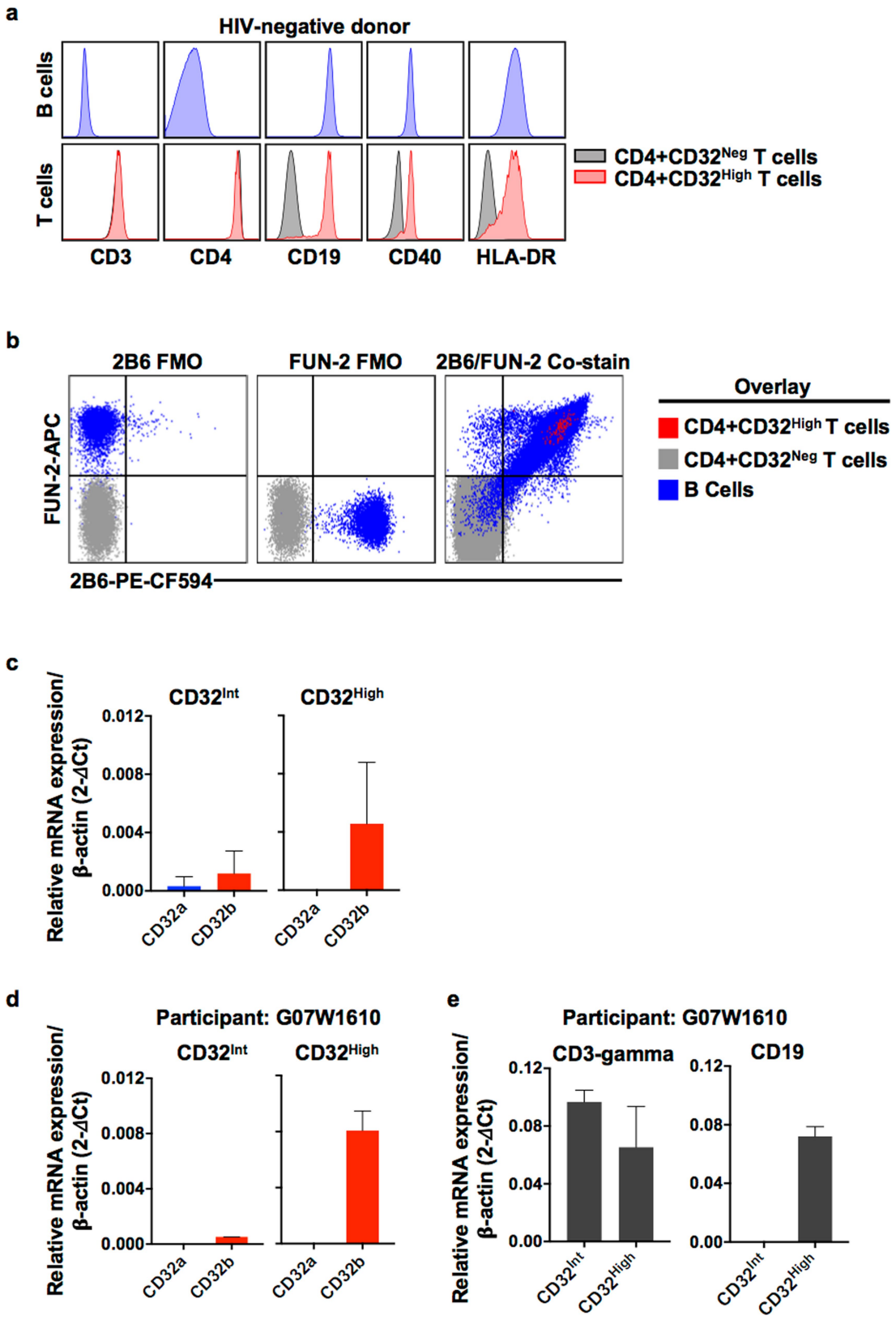

Extended Data Fig. 2 | See next page for caption.

Extended Data Fig. 2 | Detection of B cell proteins and mRNA in CD32-expressing CD4$^+$ T cells. a, CD32^{neg} and CD32^{high} (FUN-2) CD4$^+$ T cells from human PBMCs were assessed by flow cytometry for the expression of CD19, CD40 and HLA-DR, and compared to B cells (CD3$^-$ CD14$^-$CD19$^+$ lymphocytes). Representative flow cytometry results of per cell antigen levels on B cells (top, blue histograms) and CD32^{neg} and CD32^{high} CD4$^+$ T cells (bottom, grey and red histograms, respectively) from an HIV-1$^-$ donor. **b**, Representative CD32b staining of PBMCs from an HIV-1$^+$, ART-suppressed participant. PBMCs were stained with an optimized concentration of the 2B6 monoclonal anti-CD32b antibody, followed by an antibody cocktail that included the FUN-2 monoclonal pan-CD32 antibody, as described in the Methods. Shown are the 2B6 and FUN-2 fluorescence minus one (FMO) antibody cocktail-stained samples and a sample co-stained with 2B6 and FUN-2. **c**, **d**, *CD32* mRNA expression levels in CD4$^+$CD32$^+$ subsets. **c**, The relative expression of *CD32A* and *CD32B* mRNA isoforms in sorted CD4$^+$CD32^{int} and CD4$^+$CD32^{high} subsets from HIV-1$^+$, ART-suppressed participants ($n = 4$). **d**, mRNA expression of *CD32A* and *CD32B* from patient G07W1610. **e**, T and B cell lineage-specific mRNA transcripts in sorted CD4$^+$CD32$^+$ subsets from participant G07W1610. Relative mRNA expression of target genes was normalized to *ATCB* using the comparative C_t method. Results are mean ± s.d. of each value from each participant ($n = 4$; **c**), or from values generated from two separate experiments using samples from the same patient (**d**).

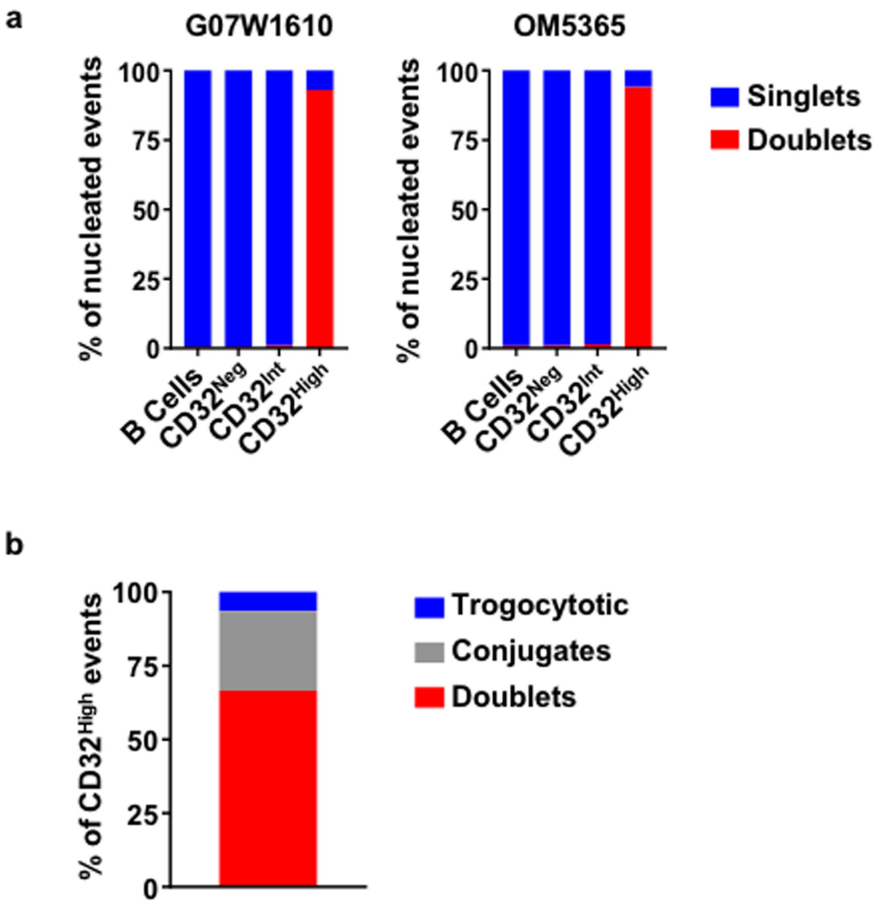

Extended Data Fig. 3 | Doublet composition of the sorted CD4^{+}CD32^{high} T cells. Sorted B cells and CD4^{+}CD32^{neg}, CD4^{+}CD32^{int} and CD4+CD32^{high} T cells from an HIV-1^{+}, ART-suppressed participant were analysed using an Amnis imaging cytometer. Singlets and doublets were quantified using the aspect ratio and nuclear staining. **a**, The proportion of total singlet and doublet events among total nucleated cells detected on the Amnis cytometer in each sorted population was determined, and is shown as individual composite bar graphs for two patients (G07W1610 and OM5365). **b**, A composite bar graph of the proportion of conjugates, doublets and trogocytotic events that comprised the sorted CD4^{+}CD32^{high} population ($n = 2$).

Extended Data Table 1 | Viral suppression of 20 HIV-1-infected participants on ART

Cohort	Participant ID	Date of Initial Suppression (MM/YY)	Length of suppression (yrs)
HEAL	HEAL-009	3/14	3
	HEAL-019	8/09	8
	HEAL-020	3/08	9.3
	HEAL-034	11/05	11.5
	HEAL-053	11/16	1
	HEAL-055	11/00	17
Maple Leaf	CIRC0024	6/98	17.0
	CIRC0133	7/08	7.0
	CIRC0196	4/14	1.2
	OM5011	11/08	6.6
	OM5148	1/08	7.5
	OM5162	9/04	10.8
	OM5203	3/12	3.3
	OM5334	7/14	0.9
	OM5365	3/08	7.3
WWH	WWH-B001	7/11	6.4
	WWH-B005	12/17	0.3
	WWH-B008	11/14	3.1
	WWH-B011	11/11	6
UPenn	G07W1610	10/05	11.8

Extended Data Table 2 | $CD4^{+}CD32^{high}$ subset proportions and HIV-1 DNA compared to total $CD4^{+}$ and $CD32^{neg}$ $CD4^{+}$ T cells

Participant ID	$CD32^{High}$			HIV-DNA enrichment		
	% in total CD4	Absolute cell count	HIV-DNA copies/cell[1]	$CD32^{High}$/ CD4 total[2]	$CD32^{High}$/ $CD32^{Neg}$[2]	$CD32^{Neg}$/ CD4 total
HEAL-009	0.007	11,427	>0.000002	0.010	0.008	1.236
HEAL-019	0.002	4,911	>0.000002	0.002	0.001	1.500
HEAL-020	0.011	8,482	>0.000002	0.008	0.008	1.036
HEAL-034	0.022	8,238	0.000426	0.199	0.212	0.937
HEAL-053	0.004	9,544	>0.000002	0.017	0.015	1.161
HEAL-055	0.011	21,806	0.00037	0.604	0.555	1.088
CIRC0024	0.015	26,200	>0.000002	0.023	0.029	0.782
CIRC0133	0.017	14,602	>0.000002	0.005	0.010	0.517
CIRC0196	0.006	5,935	0.000694	1.722	1.066	1.615
OM5011	0.008	8,862	0.001942	1.871	2.187	0.855
OM5148	0.004	8,788	0.001191	1.043	1.049	0.994
OM5162	0.016	7,133	0.000923	0.842	0.842	1.000
OM5203	0.026	12,254	>0.000002	0.021	0.011	1.911
OM5334	0.016	6,275	0.000959	0.579	0.499	1.160
OM5365	0.006	11,027	>0.000002	0.003	0.003	0.803
WWH-B001	0.020	10,922	>0.000002	0.007	0.006	1.076
WWH-B005	0.013	5,964	0.00547	0.650	0.550	1.182
WWH-B008	0.023	6,464	0.000805	0.696	0.595	1.169
WWH-B011	0.004	5,953	0.001653	1.154	1.016	1.135
G07W1610	0.012	7,984	0.002482	1.452	1.411	1.029
Median	0.012	8,635	0.000398	0.389	0.356	1.082

[1]Values below the LOD (2 copies per 10^6 cells) are shaded in grey.
[2]To calculate HIV-1 enrichment, 0.000002 was used for all values below the LOD.

nature research

Corresponding author(s): James B. Whitney

Reporting Summary

Nature Research wishes to improve the reproducibility of the work that we publish. This form provides structure for consistency and transparency in reporting. For further information on Nature Research policies, see Authors & Referees and the Editorial Policy Checklist.

Statistical parameters

When statistical analyses are reported, confirm that the following items are present in the relevant location (e.g. figure legend, table legend, main text, or Methods section).

n/a	Confirmed	
☐	☒	The exact sample size (*n*) for each experimental group/condition, given as a discrete number and unit of measurement
☐	☒	An indication of whether measurements were taken from distinct samples or whether the same sample was measured repeatedly
☐	☒	The statistical test(s) used AND whether they are one- or two-sided *Only common tests should be described solely by name; describe more complex techniques in the Methods section.*
☐	☒	A description of all covariates tested
☐	☒	A description of any assumptions or corrections, such as tests of normality and adjustment for multiple comparisons
☐	☒	A full description of the statistics including central tendency (e.g. means) or other basic estimates (e.g. regression coefficient) AND variation (e.g. standard deviation) or associated estimates of uncertainty (e.g. confidence intervals)
☐	☒	For null hypothesis testing, the test statistic (e.g. *F*, *t*, *r*) with confidence intervals, effect sizes, degrees of freedom and *P* value noted *Give P values as exact values whenever suitable.*
☒	☐	For Bayesian analysis, information on the choice of priors and Markov chain Monte Carlo settings
☒	☐	For hierarchical and complex designs, identification of the appropriate level for tests and full reporting of outcomes
☒	☐	Estimates of effect sizes (e.g. Cohen's *d*, Pearson's *r*), indicating how they were calculated
☐	☒	Clearly defined error bars *State explicitly what error bars represent (e.g. SD, SE, CI)*

Our web collection on statistics for biologists may be useful.

Software and code

Policy information about availability of computer code

Data collection	No software used.
Data analysis	We used either Graphpad Prism (version 7) or STATA (version 14). For flow cytometry analyses, we used FlowJo (version 9.9.6). For flow imaging analysis we used IDEAS (version 6.2)

For manuscripts utilizing custom algorithms or software that are central to the research but not yet described in published literature, software must be made available to editors/reviewers upon request. We strongly encourage code deposition in a community repository (e.g. GitHub). See the Nature Research guidelines for submitting code & software for further information.

Data

Policy information about availability of data

All manuscripts must include a data availability statement. This statement should provide the following information, where applicable:

- Accession codes, unique identifiers, or web links for publicly available datasets
- A list of figures that have associated raw data
- A description of any restrictions on data availability

There are no restrictions on any materials used in this study.

Field-specific reporting

Please select the best fit for your research. If you are not sure, read the appropriate sections before making your selection.

☒ Life sciences ☐ Behavioural & social sciences ☐ Ecological, evolutionary & environmental sciences

For a reference copy of the document with all sections, see nature.com/authors/policies/ReportingSummary-flat.pdf

Life sciences study design

All studies must disclose on these points even when the disclosure is negative.

Sample size	We evaluated twenty samples from HIV-1 infected virally-suppressed participants on ART and eight samples from healthy donors.
Data exclusions	No data were excluded.
Replication	All experimental findings shown in the MS were reproduced multiple times to the extent that sample availability provided. No data were used or incorporated in any figures or analyses in the manuscript if it was not reproduced more than 3 times.
Randomization	No human participants were allocated into groups.
Blinding	Technical staff were blinded throughout the study. Analyses were unblinded.

Reporting for specific materials, systems and methods

Materials & experimental systems

n/a	Involved in the study
☒	☐ Unique biological materials
☐	☒ Antibodies
☒	☐ Eukaryotic cell lines
☒	☐ Palaeontology
☒	☐ Animals and other organisms
☐	☒ Human research participants

Methods

n/a	Involved in the study
☒	☐ ChIP-seq
☐	☒ Flow cytometry
☒	☐ MRI-based neuroimaging

Antibodies

Antibodies used	Cells were stained with combinations of the following monoclonal antibodies: CD25 (M-A251), CD27 (M-T271), CD45RA (2H4 Beckman Coulter, 5H9, or HI100 Biolegend), CD14 (M5E2 or MϕP9), CD11c (S-HCL-3), CD69 (TP1.55.3 Beckman Coulter), CD66b (G10F5 Biolegend), CD19 (HIB19 Biolegend), CD56 (HCD56 Biolegend or NCAM16.2), CD4 (L200), CD8 (SK1), CD32 (FUN-2 Biolegend), CD3 (UCHT1 or SP34.2), CD86 (FUN-1), CD40 (5C3), CD32b (2B6 Creative Biolabs), and HLA-DR (L243). All antibodies are from BD Biosciences unless indicated otherwise.
Validation	All antibodies are commercially available and were commercially validated. All antibodies were also internally validated within our laboratory for specificity and cross-reactivity. Antibody validation criteria as per: http://www.nhpreagents.org/NHP/default.aspx.

Human research participants

Policy information about studies involving human research participants

Population characteristics	All HIV-1 infected virally suppressed participants were male between the age of 25 and 64 years and had been on antiretroviral therapy continuously for at least 1.8 years (range 1.8 - 23.4 yrs). All participants consented to leukapheresis at the Maple Leaf Clinic of Saint Michael's in Toronto, Canada, Whitman-Walker Heal in Washington DC, the HIV Eradication and Latency (HEAL) cohort of Brigham and Women's and Massachusetts General Hospital in Boston and the Hospital of the University of Pennsylvania in Philadelphia, respectively. Healthy donors, which include three females and five males between the age of 31 and 74 years, signed consent forms to donate samples through StemCell Technologies.
Recruitment	Patients were recruited on opportunity for existing pre-established cohorts. Coded blood samples were obtained for these studies in questioin.

Flow Cytometry

Plots

Confirm that:

☒ The axis labels state the marker and fluorochrome used (e.g. CD4-FITC).

☒ The axis scales are clearly visible. Include numbers along axes only for bottom left plot of group (a 'group' is an analysis of identical markers).

☒ All plots are contour plots with outliers or pseudocolor plots.

☒ A numerical value for number of cells or percentage (with statistics) is provided.

Methodology

Sample preparation	PBMC were isolated by Ficoll density gradient centrifugation and cryopreserved. Thawed PBMC were immediately stained with a amine viability dye, treated with an Fc Block, stained with indicated antibodies, and resuspended either in 1X PBS for sorting or in 2% paraformaldehyde for acquisition on an analyzer.
Instrument	BD LSRII analyzer, BD FACS Aria sorter, and an Amnis® ImageStreamx MKII.
Software	FlowJo (version 9.9.6) and IDEAS (version 6.2)
Cell population abundance	FACS-sorted populations were approximately 98% pure, as determined by post-sort re-runs on the Aria as well as post-sort analysis on the Amnis imaging cytometer.
Gating strategy	Sorted cells were first defined as live (amine dye negative), forward scatter (FSC) singlets, and lymphocytes (by FSC-A and SSC-A). CD4+ T cells were defined as CD3+ CD4+ and then further defined as CD32-high, CD32-low, or CD32-negative. The border between CD32-negative and CD32-low was determined by an isotype-matched control antibody. B cells were defined as CD3- CD19+.

☒ Tick this box to confirm that a figure exemplifying the gating strategy is provided in the Supplementary Information.

Descours et al. reply

REPLYING TO L. Pérez et al. *Nature* **561**, https://doi.org/10.1038/s41586-018-0493-4 (2018); C. E. Osuna et al. *Nature* **561**, https://doi.org/10.1038/s41586-018-0495-2 (2018); L. N. Bertagnolli et al. *Nature* **561**, https://doi.org/10.1038/s41586-018-0494-3 (2018)

In our previous work[1], we used an in vitro model of HIV-infected unstimulated CD4 T cells to identify CD32 as a candidate marker of HIV^+ resting CD4 T cells in vitro, and a subset of HIV^+ total CD4 T cells containing replication-competent viruses in individuals that underwent anti-retroviral therapy (ART). Of note, we did not explore the transcriptional status of hosted viruses (latent or active) ex vivo, nor the activation state of these cells (quiescent or activated)[1]. In the accompanying Comments[2–4], colleagues attempted to reproduce these findings. They present experiments that support the following conclusions: (1) the isolation of the $CD32^+$ CD4 T cell population results from artefacts caused by the flow cytometry sorting method[2,3], and (2) the sorted CD32 CD4 T cell population is not enriched in HIV nor in replication-competent proviral DNA[2–4]. Here, we formulate two questions that mirror the major issues raised by these three Comments[2–4] and discuss their results in the context of our previous report[1] and more recently published studies.

Is there any evidence that a CD4 T cell can express CD32 in the context of HIV infection? This question is raised by both Osuna et al.[2] and Pérez et al.[3]. A recent report[7], using in situ hybridization (which avoids the criticism of artefacts caused by flow cytometry sorting), showed that HIV-1 RNA co-localized with *CD32A* (also known as *FCGR2A*) RNA in 90% of examined cells in B cell follicles from four individuals. Because HIV primarily targets CD4 T cells, these data may support the ability of a CD4 T cell to upregulate *CD32* mRNA transcription after infection in vivo. Three independent groups have identified CD32 as being expressed by latently or productively infected CD4 T cells in vitro[1,5–7]. These models generated and analysed a substantial percentage of HIV-infected CD4 cells. Thus, any marker that is usually not expressed by CD4 T cells but that is detected at the surface of these cells after infection is unlikely to result from biased analyses of cellular doublets, as could be the case when working on rare events from ex vivo samples[2,3]. Instead, these data suggest that transcriptional regulation leading to the expression of CD32 mRNA and protein can probably occur after in vitro and in vivo infection of a single CD4 T cell.

Does the CD32 CD4 T cell subset contribute to viral persistence under treatment? All three of the accompanying Comments[2–4] indicate that CD32 CD4 T cells are not enriched for HIV DNA in blood. Recent work suggests, however, that in some virally suppressed HIV-infected individuals, CD32 CD4 T cells were enriched in HIV DNA, although to a lesser extent than we reported[8]. Notably, this question has been recently addressed in tissues, and results seem to be less contrasted than in blood[7,9,10] . More importantly, they revealed functional properties of these reservoir cells that have not been previously explored[7,9,10]. As discussed above, a recent report[7] found that within the B cell follicles of virally suppressed HIV-infected individuals, most of the cells containing HIV RNA and persisting despite treatment were found to express *CD32A* RNA[7]. This result seems to be in line with other data[10] that indicate that T follicular helper cells, primarily found in these territories, were enriched for HIV DNA and RNA when expressing CD32[10], although at a lower extent than our previous findings[1]. In non-lymphoid rectal tissue, CD4 T cells expressing CD32 were also enriched for both HIV DNA and RNA[9]. Notably, the co-expression of CD32 and HIV RNA reported in these two publications[9,10] suggests that CD32 marks transcriptionally active infected cells rather than latent cells. Together, these reports support the ability of CD32 to identify a subset of persistent HIV-infected CD4 T cells and suggest that they could contribute to viral persistence under ART in vivo.

In conclusion, we believe that rather than completely ruling out the relevance of CD32 for the identification of a subset of infected cells in vivo and their contribution to HIV persistence, the whole literature, including the three accompanying Comments[2–4], opens new technical challenges and questions that we should solve in the near future.

Benjamin Descours, Gael Petitjean and Monsef Benkirane are solely responsible for this Reply. The contributions of the remaining authors from the original Letter[1] were limited to recruiting patients or performing analysis on blinded samples, and thus only Descours, Petitjean and Benkirane have authored this Reply.

Benjamin Descours[1], Gael Petitjean[1] & Monsef Benkirane[1]*
[1]Institut de Génétique Humaine, Laboratoire de Virologie Moléculaire, UMR9002, CNRS, Université de Montpellier, Montpellier, France.
*e-mail: monsef.benkirane@igh.cnrs.fr

1. Descours, B. et al. CD32a is a marker of a CD4 T-cell HIV reservoir harbouring replication-competent proviruses. *Nature* **543**, 564–567 (2017).
2. Osuna, C. E. et al. Evidence that CD32a does not mark the HIV-1 latent reservoir. *Nature* **561**, https://doi.org/10.1038/s41586-018-0495-2 (2018).
3. Pérez, L. et al. Conflicting evidence for HIV enrichment in $CD32^+$ CD4 T cells. *Nature* **561**, https://doi.org/10.1038/s41586-018-0493-4 (2018).
4. Bertagnolli, L. N. The role of CD32 during HIV-1 infection. *Nature* **561**, https://doi.org/10.1038/s41586-018-0494-3 (2018).
5. Iglesias-Ussel, M., Vandergeeten, C., Marchionni, L., Chomont, N. & Romerio, F. High levels of CD2 expression identify HIV-1 latently infected resting memory $CD4^+$ T cells in virally suppressed subjects. *J. Virol.* **87**, 9148–9158 (2013).
6. Grau-Expósito, J. et al. A Novel single-cell FISH-flow assay identifies effector memory $CD4^+$ T cells as a major niche for HIV-1 transcription in HIV-infected patients. *MBio* **8**, e00876-17 (2017).
7. Abdel-Mohsen, M. et al. CD32 is expressed on cells with transcriptionally active HIV but does not enrich for HIV DNA in resting T cells. *Sci. Transl. Med.* **10**, eaar6759 (2018).
8. Martin, G. E. et al. CD32-expressing CD4 T cells are phenotypically diverse and can contain proviral HIV DNA. *Front. Immunol.* **9**, 928 (2018).
9. Hogan L. E, et al. Increased HIV- transcriptional activity and infectious burden in peripheral blood and gut-associated $CD4^+$ T cells expressing CD30. *PLoS Pathog.* **4**, e006856 (2018).
10. Noto, A., Procopio, F., Corpataux, J. M. & Pantaleo, G. $CD32^+PD\text{-}1^+$ Tfh cells are the major HIV reservoir in long-term art-treated individuals. *J. Virol.* https://doi.org/10.1128/JVI.00901-18 (2018).

Author contributions B.D., G.P. and M.B. wrote the manuscript.

Competing interests Declared none.

Additional information
Reprints and permissions information is available at http://www.nature.com/reprints.
Correspondence and requests for materials should be addressed to M.B.

https://doi.org/10.1038/s41586-018-0496-1